frontiers | Frontiers in Earth Science

TYPE Original Research
PUBLISHED 09 February 2023
DOI 10.3389/feart.2023.1104418

OPEN ACCESS

EDITED BY
Mingjun Zou,
North China University of Water Resources and Electric Power, China

REVIEWED BY
Wei Jiang,
Suzhou University, China
Yu Qi,
Yanshan University, China
Cheng Huang,
Luoyang Institute of Science and Technology, China

*CORRESPONDENCE
Yubao Shao,
yubshao@163.com
Yinghai Guo,
gyhai@163.com

SPECIALTY SECTION
This article was submitted to Economic Geology, a section of the journal Frontiers in Earth Science

RECEIVED 21 November 2022
ACCEPTED 30 January 2023
PUBLISHED 09 February 2023

CITATION
Shao Y, Wang H, Guo Y, Huang X, Wang Y, Zhao S, Zhu Y, Shen L, Huang X, Song Y, Wang M, Cui K and Yang Q (2023), Geological characteristics and gas-bearing evaluation of coal-measure gas reservoirs in the Huanghebei coalfield. *Front. Earth Sci.* 11:1104418. doi: 10.3389/feart.2023.1104418

Geological characteristics and gas-bearing evaluation of coal-measure gas reservoirs in the Huanghebei coalfield

Yubao Shao[1,2,3]*, Huaihong Wang[2,4], Yinghai Guo[1,5]*, Xinglong Huang[2,3,6,4], Yongjun Wang[2,3,6,4], Shushan Zhao[2,3,6,4], Yuzhen Zhu[2,3,6,4], Lijun Shen[2,3,6,4], Xin Huang[2,3,6,4], Yu Song[2,3,6,4], Ming Wang[2,3,6,4], Kai Cui[2,3,6,4] and Qidong Yang[2,3,6,4]

[1]School of Resources and Geosciences, China University of Mining and Technology, Xuzhou, China, [2]Shandong Provincial Research Institute of Coal Geology Planning and Exploration, Jinan, China, [3]Shandong Research Center for Accident Prevention Technology in Key Industries (Non coal Mines), Jinan, China, [4]Key Laboratory of Coal Geophysics, Chinese Geophysical Society, Jinan, China, [5]Key Laboratory of Coalbed Methane Resources and Reservoir Formation Process, Ministry of Education, China University of Mining and Technology, Xuzhou, China, [6]Technical Innovation Platform for Unconventional Energy Exploration in Shandong Province, Jinan, China

Bystudying the source reservoir geochemical characteristics, reservoir cap physical properties, gas-bearing characteristics and reservoir-forming types of the coal-measure gas (CMG) accumulation system, the potential of CMG resources in the Huanghebei Coalfield was determined, and the sedimentary reservoir control mechanism was analyzed, which is of great significance for the orderly development of CMG reservoirs. CMG in the Huanghebei Coalfield mainly includes abundant shale gas (SG; 2100.45 × 10^8 m^3), coalbed methane (CBM; 137.89 × 10^8 m^3) and a small amount of tight sandstone gas, limestone gas and magmatic rock gas. CMG rocks mainly include shale and coal seams of the marine–terrestrial transitional facies Taiyuan Formation and continental facies Shanxi Formation, providing a favorable material basis for CMG enrichment. The coal seams are largely mature to highly mature, with satisfactory hydrocarbon generation potential and reservoir connectivity. They are low-porosity, low-permeability, underpressurized and undersaturated reservoirs. The shale organic matter is primarily Type II, with a moderate organic matter abundance. The material is at the middle-to high-maturity stage, provides a suitable hydrocarbon generation potential, belongs to low-porosity and low-permeability reservoirs, and exhibits favorable fracturing properties. There are several stable and independent gas-bearing systems among the coal measures. The CMG accumulation combination types are mostly self-sourced gas reservoirs and self-sourced+other-source near-source gas reservoirs, followed by other-source gas reservoirs. CBM and SG play the role of vertical regulation and horizontal regulation, respectively.

KEYWORDS

Huanghebei Coalfield, coal-measure gas, Taiyuan Formation, Shanxi Formation, reservoir feature, gas-bearing evaluation, gas reservoir assemblage

1 Introduction

Coal-measure gas (CMG) refers to natural gas generated from coal, carbonaceous shale and dark shale in coal measures, including shale gas (SG), coalbed methane (CBM) and tight gas (TG) (Law and Curtis, 2002; Clarkson, 2013; Dai, 2018; Hou et al., 2018; Zou et al., 2019; Shen et al., 2021; Li et al., 2022). In recent years, due to progress in exploration and development technology, CMG has changed the global natural gas pattern and plays an important role in ensuring the world energy supply and reducing air pollution. The typical CMG basins worldwide mainly include the San Juan Basin in the United States, the Surat Basin in Australia, the Western Siberian Basin in Russia and the Ordos Basin in China, but there is no independent resource evaluation of CMG abroad (Zou et al., 2019). Based on the spatial ranges and vertical extents of CMG overlap, the analysis of CMG as a unified gas-bearing system has therefore become a key research direction (Qin, 2021).

CMG constitutes an important guarantee for increasing reserves and producing natural gas in China (Qin, 2021). According to a recent prediction of the China Geological Survey, the CMG resources in China total approximately 82×10^{12} m^3 (Bi, 2019). China has become the sixth largest gas-producing country globally, evolving from being a gas-poor country (Dai, 2018). By the end of 2016, the discovered coal-measure fields in China accounted for 66% of the national gas fields, mainly distributed in the Ordos, Qinshui, Sichuan and other Carboniferous–Permian basins and Jurassic–Cretaceous coal-bearing basins, such as Tarim and Qaidam, as well as the Yinggehai-Qiongdongnan and Donghai Cenozoic coal-bearing basins (Zou et al., 2019). CMG is derived from the same origin and coexists in multiple layers, and it is generally associated with strong hydrocarbon generation, high continuous filling capacity, coexistence of multiphase gas, multiple types of gas reservoirs, source reservoir facies dependence, reservoir cap interaction, multiple seals, complex gas–water distribution relationships, and fragile dynamic balance between systems (Fu et al., 2013; Yang et al., 2013; 2015; Cao et al., 2014; Yuan, 2014; Qin et al., 2016; Zheng, 2016; Qin, 2018; 2021; Bi et al., 2020; Liu et al., 2020; Bi et al., 2021). The accumulation of CMG mainly depends on four aspects: hydrocarbon generation intensity, migration mode and transport system, formation fluid energy, and regional effective caprock. The accumulation effect of superimposed gas-bearing systems has become a leading direction of coal-measure gas geological research (Qin, 2018), which can provide a theoretical basis for large-scale exploration and development.

The exploration of upper Paleozoic coal-formed gas reservoirs in the Bohai Bay Basin adjacent to the northern Huanghe North coalfield has made great breakthroughs (Jin et al., 2009; Liang et al., 2016), indicating that the study area has good exploration potential. The Huanghebei area is a typical coal-bearing basin east of the coal accumulation area in North China, which is affected by intrusions associated with Yanshanian magmatism. It shows the unique characteristics of coalbed methane, shale gas and a skarn-rich iron ore pool (ore) (Wang et al., 2021). The abundance of organic matter in the Carboniferous-Permian coal measure source rocks in the study area is poor to medium (Cui, 2001; Chen et al., 2003; Yu, 2003; Mu, 2008). The peak period of gas generation was mainly in the Early Triassic and Jurassic-Cretaceous, and the abnormally high thermal geothermal field in the Yanshanian played a key role in the hydrocarbon generation of the source rocks (He et al., 2005; Zhao, 2005; Li, 2006; Zhou, 2015; Yang et al., 2018). These source rocks still retain a high hydrocarbon generation potential (Xu et al., 2005). The occurrence of coal-measure gas is mainly affected by factors such as faults, sedimentary environment, inorganic minerals, caprock conditions, burial depth, overburden thickness, hydrogeological conditions and magma (Fan et al., 2001; Liu and Guo, 2003; Zhao, 2007; Zhao et al., 2016; Huang et al., 2018; Li, 2019). Shallow CBM has been pumped and utilized in the study area. In 2010, the Zhaoguan Coal Mine used the gas pumped during coal mining for power generation for the first time in this area, which indicates that CMG here could yield a certain development prospect. With the support of the Shandong Provincial Geological Exploration Fund, survey and evaluation studies of CBM and SG resources in the research area have been conducted. A number of gas-bearing strata have been found in the Upper Paleozoic Taiyuan Formation and Shanxi Formation. CMG is dominated by CBM and SG, demonstrating the characteristics of source reservoir facies dependence, reservoir cap interaction and multiple seals. In this paper, the coal seams and shale of the upper Paleozoic Shanxi Formation and Taiyuan Formation were adopted as research objects, and a systematic study of the reservoir formation and exploration potential of the Huanghebei Coalfield is of great significance to understanding the CMG reservoir formation mechanism and to the collaborative exploration and efficient development and utilization of multiple mineral resources.

2 Geological setting

2.1 Regional structure and stratigraphic characteristics

The Huanghebei Coalfield is located in the western regions of the Luxi uplift in the North China Plate (Figure 1). It starts from the Woniushan fault in the east, reaches the Liuji fault in the west, is bounded by the outcrop of the bottom (hidden) of the coal-bearing stratum in the south, and ends at the Qiguang fault in the north (Figure 1). This area is rich in coal resources and is an important coal production base in western Shandong Province. The study area generally comprises a wide and gentle monocline trending northeast–northwest, which is shallow in the south and deep in the north. The dip angle of the monocline is generally low, with wide and gentle northeast-trending folds developed. The regional structure is dominated by fault structures. In general, there are three groups of fault structures distributed along the NE–NNE, NW–NNW, and near-E–W directions, and the former two groups are relatively well developed, while SN-directed faults are not very developed in this area. These groups of large faults intersect each other, controlling the generation and development of uplift and depression in the region.

The stratigraphic division of the study area is classified as the western Shandong stratigraphic division of the North China stratigraphic area. Only a small range of Cambrian Ordovician strata is exposed in the south (south of the Huanghebei Coalfield), and the remaining area is covered by Quaternary strata. The strata from old to new include the Taishan Group and Cambrian, Ordovician, Carboniferous, Permian, Triassic, Neogene and Quaternary strata, lacking Upper Ordovician to Lower Carboniferous, Jurassic and Cretaceous strata. Paleogene rocks are not developed to the south of the Qiguang fault, and they are mainly distributed to the north of the Qiguang fault.

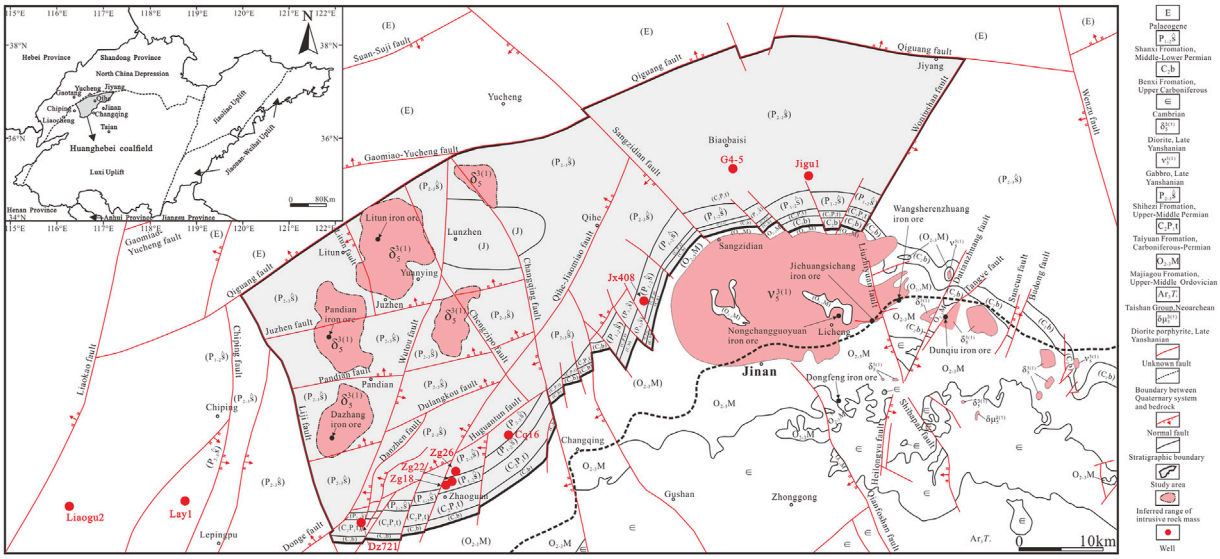

FIGURE 1
Geological map of the pre-Neogene bedrock in the study area. The area north of the dotted line at the lower right is the Quaternary coverage area. The overview map at the upper left shows the location of the study area, and the gray area within the black line denotes the Huanghebei Coalfield.

Magmatic rocks are widely distributed in the region, mainly including Neoarchean, Mesoproterozoic and Mesozoic intrusive rocks. Among them, Neoarchean intrusive rocks are the most developed and are distributed in the southern part of the Zhangqiu–Changqing area. Ultrabasic, basic, and acidic intrusive rocks occur, with intermediate–acidic intrusive rocks being the most common. The distribution of Mesozoic intrusive rocks is limited, and these rocks are mainly distributed in the Yucheng - Jinan area and are mainly composed of intermediate–basic rocks (Figure 1). Magmatic rocks of other ages are not developed. The Mesozoic intrusive rocks, such as the Jinan gabbro (Yang et al., 2005; Huang et al., 2012; Yang, 2012; Ning et al., 2013; Xie et al., 2015), Tai'an gabbro and diorite (Ning et al., 2013), and Qihe—Yucheng diabase (Zhu et al., 2021), mainly formed in the Early Cretaceous (100 ~ 135 Ma). The intrusive rocks in the study area are mainly diabase, diorite, quartz monzodiorite, quartz monzonite and granite. Among them, the Litun rock mass contains all the above rock types (Shen et al., 2020; Shen et al., 2021; Zhu et al., 2021), while the Dazhang rock mass and Pandian rock mass mainly contain quartz monzonite (Zhang et al., 2022). Except for the Litun rock mass, which exhibits a narrow range of direct contact with the overlying Neogene strata, the known rock groups in the west are capped by residual Permian strata, and the Jinan rock mass occurs in direct contact with Quaternary strata except for a small amount of Ordovician limestone. At the same time, three layers of Mesozoic magmatic rocks intruded the Shanxi Formation and Taiyuan Formation, and these magmatic rocks are present in the form of bedrock or dikes. The upper and lower layers are acidic magmatic rocks, and the middle layer comprises medium-basic magmatic rocks. The layers intruded by the upper magmatic rock are mainly coal seams three and four overlying strata of the Shanxi Formation. The middle magmatic rock mainly intruded coal seam five of the Shanxi Formation to coal seam nine of the Taiyuan Formation and severely damaged coal seam seven of the Taiyuan Formation. The lower magmatic rock mainly damaged coal seams 11 and 13 of the Taiyuan Formation.

2.2 Sequence stratigraphic characteristics

CMG in China exhibits the characteristics of large-scale vertical and horizontal distributions, an unclear gas-water boundary, a complex pressure system, diverse reservoir rock types, interbedded occurrence, notable cyclicity, and variable source–reservoir–cap associations (Qin, 2021). The CMG characteristics in the study area are consistent with the basic geological characteristics of China. The proposal of an unconnected multiple superimposed CBM system explains the highly consistent relationship and genetic mechanism between sequence division and independent segmentation of the gas content gradient in the sequence stratigraphic framework (Qin et al., 2008; Shen et al., 2012) and further extends to the superimposed CMG-bearing system. The sequence stratigraphic framework explains the development of key layers and establishes a coal measure reservoir (production) combination model constrained by these key layers. High-resolution identification of fluid and energy under the cell framework of three-layer sequence stratigraphy was carried out (Qin et al., 2016; Shen et al., 2017). The logging data of wells Zg18, Zg22 and Zg26 demonstrate that SG, CBM and a small amount of TG, carbonate rock gas and magmatic rock gas occur in the Shanxi Formation and Taiyuan Formation (Figure 2), which are constrained by the sequence stratigraphic framework and contain multiple relatively independent gas-bearing units.

The isochronous sequence stratigraphic framework is helpful for predicting the distribution of coal measure source rocks (Shao et al., 2008). For the offshore coal-bearing rock series of the North China platform, three third-order sequences can be identified in the Benxi Formation, Taiyuan Formation and Shanxi Formation (Shao et al., 2014). There are two scales of the sequence stratigraphic division

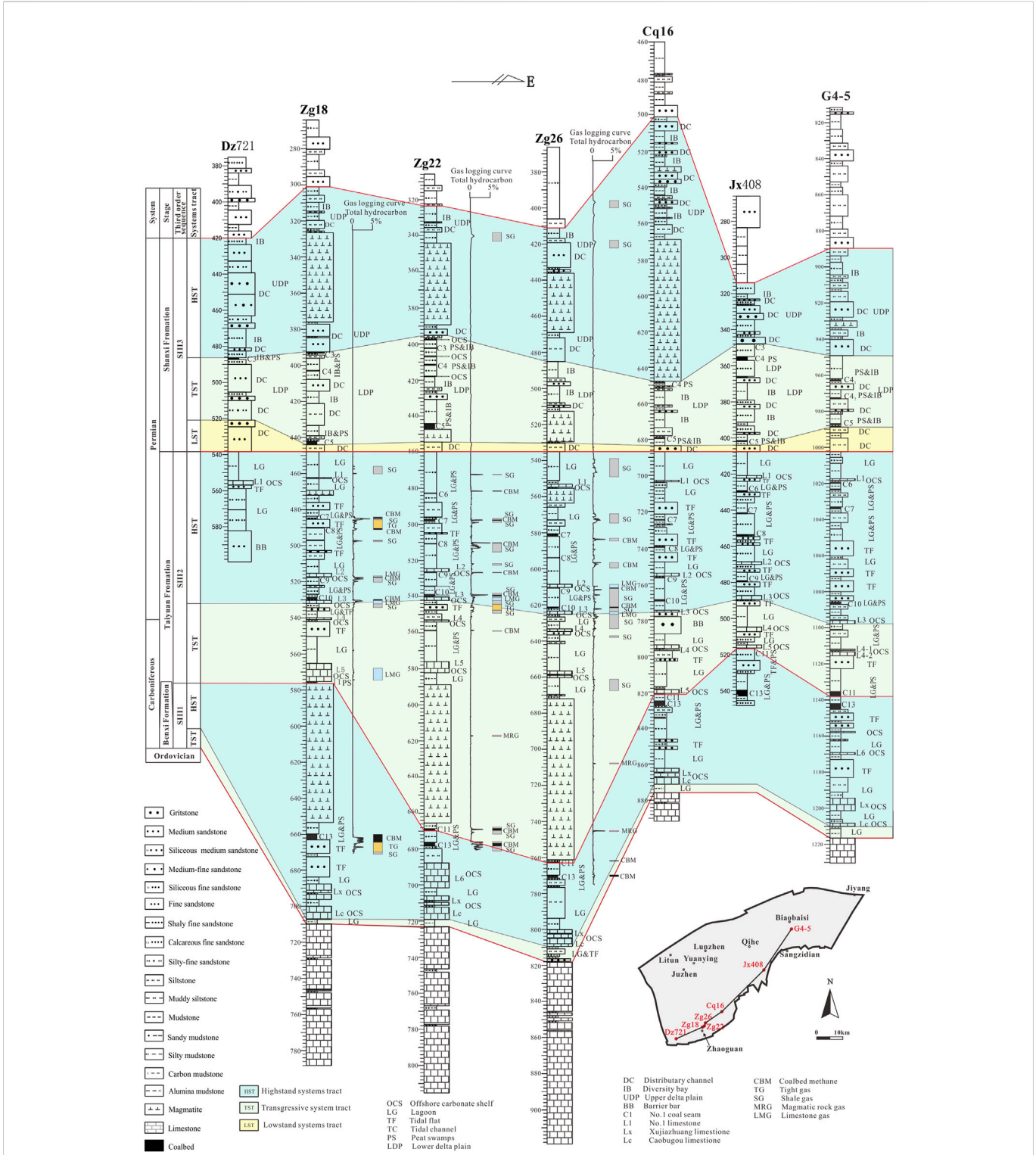

FIGURE 2
Correlation diagram of the sedimentary facies and sequence stratigraphy (SW–NE).

scheme of the Benxi Formation, Taiyuan Formation and Shanxi Formation in Shandong Province, including three third-order sequences (Wang et al., 2003; Li et al., 2005; Zhang et al., 2010; Li et al., 2021) and four third-order sequences (Jia and Lv, 2009). According to the regional unconformity surface and the regional tectonic stress transformation surface, the Permian Shanxi Formation, upper Carboniferous–lower Permian Taiyuan Formation and Carboniferous Benxi Formation in the study area are divided into three third-order sequences (SIII1-SIII3) and eight fourth-order sequences (SIV1-SIV8) (Figure 2). The Shanxi Formation corresponds to sequence SIII3, the Taiyuan Formation corresponds to the highstand systems tract (HST) of sequence

SIII1 and sequence SIII2, and the Benxi Formation corresponds to the transgressive systems tract (TST) of sequence SIII1. The bottom boundary of sequence SIII1 is a regional unconformity surface, namely, the interface between Ordovician and Carboniferous strata. The maximum flooding surface is the boundary between the Taiyuan and Benxi Formations, which is located at the bottom of the Xuhui Formation. Thirteen coal seams are mainly developed in the TST. The bottom boundary of sequence SIII2 mainly comprises the floor of the No. 11 coal seam below the L5 limestone formed in a lagoon and swamp environment. The maximum flooding surface is located at the bottom of the L3 limestone. The No. 6, 7, 8, 9, 10 and 11 coal seams of the Taiyuan Formation are well developed. The initial flooding surface of sequence SIII3 is located near the floor of the No. 5 coal seam, and the maximum flooding surface is located at the top of the No. 3 coal seam. The bottom boundary of the sequence mainly encompasses the incised valley of the distributary channel in the lower delta plain, which is the boundary between the Shanxi Formation and Taiyuan Formation. The No. 3, 4, and 5 coal seams of the Shanxi Formation are well developed.

2.3 Evolution of the sedimentary system

The Carboniferous–Permian coal accumulation basin in North China mainly developed in the paleogeographic background of sea–land interaction (Liu et al., 1987; Ma and Tian, 2006). The western Shandong region mainly featured carbonate platform, lagoon tidal flat, and shallow water delta sedimentary systems from Benxi to Shanxi (Wang et al., 2003; Jia and Lv, 2009; Zhang et al., 2010; Shao et al., 2014). In the late Paleozoic, namely, from the Carboniferous to the Permian, barrier lagoon, tidal flat, river-controlled shallow-water delta and river–lake sedimentary systems were mainly developed in the study area (Wang et al., 2021). Along with the North China Depression, the study area has experienced large-scale transgression since the late Carboniferous, formed coal-bearing rock series represented by sand–mud interbeds, and developed favorable gas reservoirs. During the Benxi period, with seawater intrusion, the TST of sequence SIII1 formed lagoon tidal flat deposits dominated by gray–white bauxite and gray or gray–black mudstone with thin bedded limestone interbedded residues, accompanied by small-scale transgression. During the Taiyuan period, at the end of the late Carboniferous, the North China Depression experienced a movement entailing a rise in the north and a descent in the south. By this time, the epicontinental sea environment had reached its peak. The HST of sequence SIII1 and sequence SIII2 developed an offshore shelf barrier lagoon tidal flat sedimentary system. The lithology mainly includes dark mudstone, fine siltstone, thin limestone and coal seams. The biological species are rich, and the organic content is high. During the Shanxi period, with tectonic uplift and seawater retreat, a fluvial-dominated shallow delta depositional system was widely developed in sequence SIII3, with distributary channels and interdistributary bays occupying the main part, in which the lowstand systems tract (LST) and TST mainly comprise a set of shallow delta–lower delta plain deposits, while the HST mainly includes shallow water delta–upper delta plain and meandering river deposits. During the Shihezi period, the Huanghebei Coalfield completely transformed from epicontinental sea deposits to continental deposits, and seawater was withdrawn. At this time, a set of very thick silicate clastic materials were deposited. The Huanghebei Coalfield experienced the complete process of the formation, development, prosperity, shrinkage and transformation of the epicontinental sea basin during the late Paleozoic and experienced multiple transgression regression cycles. The lithofacies paleogeographic pattern accordingly changed and was subjected to the evolution process of the tidal flat–barrier lagoon system–delta system–river system. During this period, a complete set of coal-measure source rocks in the Shanxi Formation and Taiyuan Formation with large thicknesses and high organic contents were developed, and this sequence comprises a vertical succession of shale, coal seam, clastic rock and carbonate rock strata and provides the basic geological conditions for a CMG source, reservoir and cap.

3 Samples and experiments

3.1 Samples

Our samples were mainly collected from five wells, Zg18, Zg22, Zg26, Cq16 and Lay1, constructed in 2011–2016. Three coal samples and 12 shale samples were collected from Well Zg18. Three coal samples and five shale samples were collected from Well Zg22. Four coal samples and 12 shale samples were collected from Well Zg26. Thirty-six shale and six coal seam samples were collected from Well Cq16. Twenty-two shale and 11 coal seam samples were collected from Well Lay1. Field tests and laboratory analyses were carried out immediately after sample collection.

3.2 Experimental approaches

Maceral identification, macroscale coal rock type identification, microfracture statistics, gas content analysis, isothermal adsorption tests, and total organic carbon analysis of coal seam samples were performed at the Shandong Taishan Mineral Resources Detection and Research Institute.

The coal macerals were determined according to the determination of coal group composition and minerals in coal (GB/T 8899-2013). The volume fraction of various macerals was determined by using the number point method under axio scope. A1 microscope (Carl Zeiss, Germany) and under single polarized light or incomplete orthogonal polarized light to determine the type of organic matter. The macroscopic coal rock type as mainly determined by axio scope. A1 microscopy based on the classification of macrolithotype for bituminous coal (GB/T 18023-2000). Refer to the description methodology of fractures in coal (MT/T 968-2005) for information on the observation and statistics of coal microfractures.

The coal seam gas content was determined according to the method of determining coalbed gas content (GB/T 19559-2008). The time from drilling to coring is required to be no more than 2 min for core lifting every 100 m. An 800 g sample of core was canned within 10 min after the core reached the wellhead, and the desorption capacity was tested in a thermostatic water bath. Natural desorption ended after the daily desorption capacity was less than 10 cm^3 for seven consecutive days. The desorbed sample was pressed to 2-3 cm, and 500 g was placed into a ball mill for residual gas measurement. At the time of rapid gas measurement, a 500 g sample of coal core was loaded into the ball mill tank. First, it was naturally desorbed for 8 h

and then crushed by ball milling for 30 min. Then, it was put into the thermostatic device for natural desorption. The process of crushing and desorption was repeated until the amount of desorbed gas over two consecutive times was less than 10 cm^3. The measured gas volume of natural desorption and residual gas was converted into the total gas content at a temperature of 0°C and a pressure of 101.325 kPa, with correction for gas loss. The gas components mainly include CH_4, CO_2, N_2 and heavy hydrocarbons, using GC-7820 gas chromatograph (Shandong Huifen Instrument Co., Ltd., China). The analysis of natural gas by gas chromatography (GB/T 13610-2003) was used for the test process. Three gas component analysis samples were collected for each desorption sample during the test on the first, third and fifth days of desorption. Samples with a low coalbed methane content were collected appropriately in advance.

The coal seam isothermal adsorption test used the WX-VI high-pressure isothermal adsorption apparatus (Qingdao Ruihai Xinda Instrument Co., Ltd., China). According to the method of determining microscopically the reflectance of vitrinite in coal (GB/T 19560-2008) and determination of equilibrium moisture in coal isothermal adsorption method (MT/T 1157-2011), 200 g coal samples with particle sizes of 0.25–0.18 mm were prepared, and a sample mass of 40 g was weighed for equilibrium moisture measurement. Six test pressures (0.5, 1.0, 2.0, 4.0, 6.0, and 8.0 Mpa) were applied. Then, the Langmuir pressure (P_L) and Langmuir volume (V_L) were obtained.

The reflectance of coal seam vitrinite was measured by axio scope. A1 microscope (Carl Zeiss, Germany) at the Shandong Taishan Mineral Resources Testing and Research Institute and the laboratory of the Guizhou Coalfield Geology Bureau. Referring to the method of determining microscopically the reflectance of vitrinite in coal (GB/T 6948-2008) (λ= 546 nm) measured by a photoelectric converter, more than 50 points were measured for single coal seam coal samples when the maximum reflectance of vitrinite was 0.45%–2.00%, and more than 100 points were measured when the maximum reflectance of vitrinite was 2.00% to ensure sufficient accuracy.

Coal seam permeability and reservoir pressure were determined by the Xi'an Research Institute of China Coal Research Institute with reference to the method of injection/falloff well test for coalbed methane well (GB/T 24504-2009). After drilling to the floor of the tested coal seam, the test string was inserted at the roof of the coal seam, and a microfracture test was conducted to obtain the maximum injection pressure value. Then, an injection/pressure drop test was performed. The water injection time was 18 h, and the well shut-in time was 36 h; then, *in situ* stress tests were carried out.

The gas content, porosity, permeability, pyrolysis analysis, total organic carbon, and mechanical properties of shale were measured at the Shandong Taishan Mineral Resources Detection and Research Institute.

The gas content of shale was determined according to the measurement method of shale gas content (SY/T 6940-2013). The time from drilling to coring was required to be less than 12 h. A core sample with a height of 20 cm–30 cm was canned within 10 min after the core reached the wellhead. The desorption was tested in a thermostatic water bath until the daily desorption volume was less than 5 cm^3 for three consecutive days. Three samples after desorption, 100 g each, were placed into the sealed tank of the residual gas volume tester for crushing, and the residual gas volume was taken as the mean value of the measurement results of the three samples. The measured gas volume of natural desorption and residual gas was converted into the total gas content at a temperature is 0°C and a pressure of 101.325 kPa, with correction for gas loss.

The porosity and permeability of shale were measured by a CMS-300 automatic core overburden porosity-permeability tester (Beijing Aotao Science & Technology Co., Ltd., China) with reference to porosity and permeability measurement under overburden pressure (SY/T6385-1999). The overburden pressure was applied to the rock sample by means of hydrostatic pressure to ensure that the stress in all directions of the rock sample was balanced and the pore pressure remained unchanged. The overburden pressure was gradually increased to measure the porosity and permeability. The accuracy of the pressure sensor and the relative error of the helium pore meter are both less than 0.1%.

The pyrolysis analysis of shale was measured by YY-3000A oil shale comprehensive evaluator (Lunan Ruihong Chemical Instrument Co., Ltd., China) according to the reference standard rock pyrolysis analysis (GB/T18602-2012). The sample was crushed to a particle size of 0.07–0.15 mm, an analytical balance with an accuracy of 0.1 mg was used to weigh 0.1 g, and the sample was placed into the instrument for heating. The sample was pyrolyzed in a nitrogen environment with a purity of >99.99% at 90°C, 300°C, and >300°C–600°C. The measured parameters include the hydrocarbon content (S_0) measured at 90°C, the hydrocarbon content (S_1) measured at 300°C, the hydrocarbon content (S_2) measured at >300°C–600°C, and the temperature at the highest point of the corresponding *S2* peak (T_{max}).

The compressive strength, elastic modulus, Poisson's ratio and tensile strength of shale was determined by a YAW-300D microcomputer controlled compression and bending tester, WAW-600F microcomputer controlled electro-hydraulic servo rock testing machine and YAW-1000D microcomputer controlled compression shear testing machine (Jinan Xinshijin Test Machine Co., Ltd., China). The compressive strength was tested according to methods for determining the physical and mechanical properties of coal and rock-Part 7: methods for determining the uniaxial compressive strength and counting softening coefficient (GB/T 23561.7-2009). Elastic modulus and Poisson's ratio was determined according to methods for determining the physical and mechanical properties of coal and rock-Part 8: methods for determining the deformation parameters of coal and rock (GB/T 23561.8-2009). Refer to methods for determining the physical and mechanical properties of coal and rock-Part 10: methods for determining tensile strength of coal and rock (GB/T 23561.10-2010).

The determination of total organic carbon in coal seams and shale was based on the specification for determination of total organic carbon in sedimentary rock (GB/T18602-2012), using CS230 carbon sulfur analyzer (LECO, United States). The sample was ground until the particle size was less than 0.2 mm. An analytical balance with an accuracy of 0.1 mg was used to weigh 1 g of the sample. The inorganic carbon in the sample was removed with dilute hydrochloric acid, and the sample was burned under a high-temperature oxygen flow to convert the total organic carbon into carbon dioxide. The content of total organic carbon was determined by infrared detection.

The shale kerogen macerals were determined in the laboratory of Guizhou coalfield geology bureau using a axio scope. A1 microscope (Carl Zeiss, Germany). According to method of identification microscopically the macerals of kerogen and indivision the kerogen type by transmitted-light and fluorescence (SY/T 5125-2014), each maceral was identified according to optical characteristics under

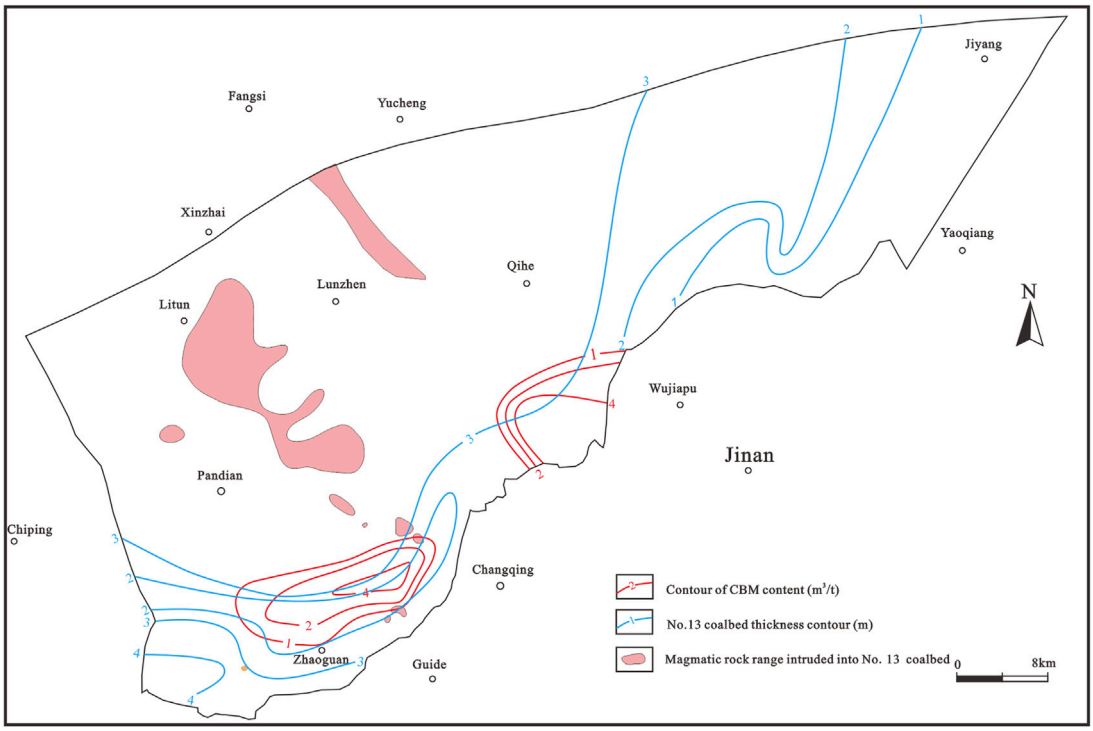

FIGURE 3
No. 13 coalbed thickness and gas content distribution.

transmitted light and emission fluorescence, and the contents of the sapropel group, chitin group, vitrinite group and inertinite group were obtained. The type index (*TI*) was calculated, and the types of kerogen were classified.

The vitrinite reflectance of shale was measured in the laboratory of the Guizhou coalfield geology bureau with a axio scope. A1 microscope (Carl Zeiss, Germany). According to method of determining microscopically the reflectance of vitrinite in sedimentary (SY/T5124-2012), for the optical sheet of the same sample, when the average reflectivity is greater than 2.0%, the number of measured points should greater than 30; when the average emissivity is between 0.5% and 2.0%, the number of measured points should greater than 20 to ensure the representativeness of the measured results.

4 CMG accumulation system

4.1 Development characteristics of the coal-measure source rocks

The shale and coal seams of the Taiyuan Formation and Shanxi Formation are the main coal-bearing gas source rocks in the study area, which exhibit the characteristics of extensive deposition. The total thickness of the coal-bearing strata of the Taiyuan Formation and Shanxi Formation in the study area is approximately 245 m. There are 14 coal seams in the coal-bearing strata, of which the No. 1 to 5 coal seams occur in the Shanxi Formation, and the No. 6 to 14 coal seams occur in the Taiyuan Formation. The minable and partially minable coal seams are the No. 5, 6, 7, 8, 10, 11 and 13 coal seams. The total thickness of the coal seams varies between 4 and 9 m, with an average of 5.5 m. The coal-bearing coefficient of the minable coal seams is 2.2%, revealing thin characteristics in the eastern and northern parts and thick characteristics in the western and southern parts in the study area. For example, the thickness center of the No. 13 coal seam is mainly located in the southwest of the Huanghebei Coalfield (Figure 3). The spatial distribution of each coal seam is deep in the north and shallow in the south, ranging from −200 to −2500 m.

Among them, sandstone is mainly developed above the No. 4 coal seam in the Shanxi Formation and is greatly affected by the intrusion of upper magmatic rock. Under the influence of lower magmatic rocks, shale below the No. 11 coal seam in the Taiyuan Formation is damaged to varying degrees, which is unfavorable for CMG accumulation. There are favorable SG intervals with large cumulative thicknesses in the strata between the No. 4 coal seam of the Shanxi Formation and the No. 10 coal seam of the Taiyuan Formation. The gas logging results for the corresponding intervals in Wells Zg18, Zg22 and Zg26 are satisfactory. The accumulated thickness of dark shale in the area ranges from 52.83 to 97.1 m, with an average of 84.8 m. The thickness in the south–central part of the area is small, mostly less than 60 m, while the thickness in the northwestern part is large, mostly greater than 90 m. The burial depth ranges from 414.05 to 1290.55 m, which is deep in the north and shallow in the south.

4.2 Organic geochemical characteristics of the coal-measure source rocks

Organic matter in source rock is the main factor determining the hydrocarbon generation ability. The organic matter abundance

TABLE 1 Evaluation results of the organic matter abundance of marine terrestrial interactive shale.

Well number	Layer	Number of samples	Hydrocarbon source rock evaluation results (the evaluation parameters refer to Huang et al. (1996)			
			Good-excellent	Medium	Poor	Non
			TOC: 3%–40%	TOC: 1.5%–3%	TOC: 0.6%–1.5%	TOC:<0.6%
Cq16	Shanxi Formation	7	1	4	1	1
	Taiyuan Formation	28	4	12	18	1
Lay1	Shanxi Formation	3	2	0	0	1
	Taiyuan Formation	19	3	14	2	0
Well	Stratum	Number of samples	S_1+S_2: 6.0–200 mg/g	S_1+S_2: 2.0–6.0 mg/g	S_1+S_2: 0.5–2.0 mg/g	S_1+S_2: <0.50 mg/g
Cq16	Shanxi Formation	7	0	0	1	6
	Taiyuan Formation	29	2	5	19	3
Lay1	Shanxi Formation	3	2	0	0	1
	Taiyuan Formation	18	1	6	10	1

indexes of marine-terrigenous source rocks widely recognized by the academic community mainly include the total organic carbon (TOC) content and hydrocarbon generation potential (S_1+S_2) (Huang et al., 1996). Based on the above indicators, the organic matter abundance of shale in the study area was evaluated (Table 1).

4.2.1 Abundance of organic matter

In the study area, the S_1+S_2 value of the coal seams of the Shanxi Formation and Taiyuan Formations in Well Jigu one varied between 80.93 and 173.68 mg/g, with an average of 132.95 mg/g, and the hydrogen index (HI) ranged from 133.84 to 188.00 mg/g, with an average of 161.67 mg/g (Chen et al., 2003; Yu et al., 2003). The TOC mainly refers to the data of adjacent Well Lay1, in which the TOC content in the Shanxi Formation ranged from 62.4% to 73.65%, with an average of 67.00%. The TOC content in the Taiyuan Group varied between 58.3% and 76.65%, with a mean of 67.34%.

The TOC content in the shale of the Shanxi Formation in Well Cq16 varied between 0.43% and 3.25%, with an average of 2.03%; S_1+S_2 varied between 0.1 and 0.78 mg/g, with an average of 0.27 mg/g; the TOC content in the shale of the Taiyuan Formation ranged from 0.55% to 17.65%, with an average of 2.82%; and S_1+S_2 ranged from 0.3 to 17.45 mg/g, with an average of 2.44 mg/g. Moreover, the TOC content in the Shanxi Formation shale in Well Lay1 in the adjacent area ranged from 0.57% to 18.25%, with an average of 9.49%, and S_1+S_2 ranged from 0.3 to 31.10 mg/g, with an average of 16.93 mg/g. The TOC content in the shale of the Taiyuan Formation varied between 1.11% and 21.95%, with an average of 3.98%, and the S_1+S_2 value ranged from 0.35 to 8.72 mg/g, with an average of 2.02 mg/g. As indicated by the statistical results (Table 1), the shales of the Shanxi Formation and Taiyuan Formation in Wells Cq16 and Lay1 mainly included poor to medium hydrocarbon source rocks. Combined with the inversion data of coal exploration well logging in the area, the TOC content in the shale of the Shanxi Formation and Taiyuan Formation in the study area ranged from 1.78% to 2.74%, with an average of 2.09%. The overall assessment of the organic matter abundance suggested a moderate abundance. The central area is a high-value area, with a TOC content higher than 2.6%, and the value gradually decreases toward the surroundings.

Both coal and shale seams are the main gas-generating layers of hydrocarbon source rocks, in which coal seams, as accumulated organic matter, contribute more to hydrocarbon generation and fulfill a decisive role in CMG reservoirs, while shale rich in organic matter remains stable during development, and the thickness advantage compensates for the lack of organic matter. It has been found that the hydrocarbon generation capacity of exinite source rocks with a certain content is higher (Qin et al., 2005). In general, the Huanghebei coalfield exhibits favorable hydrocarbon generation conditions.

4.2.2 Maturity of organic matter

Affected by magmatic intrusion, the vitrinite reflectance (R_o) values in the coal reservoirs of the Shanxi Formation and Taiyuan Formation in the area ranged from 0.61% to 6.35%, which suggests the mature to highly mature stage, and were higher than those of Well Lay1 in the adjacent area not affected by magmatic intrusion (with R_o ranging from 0.70% to 0.74%).

The shale R_o value of the Shanxi Formation in Well Cq16 ranged from 2.11% to 2.44%, T_{max} ranged from 471.9°C to 476.4°C, the shale R_o value of the Taiyuan Formation ranged from 1.34% to 2.13%, and T_{max} reached 476.40°C. The shale mainly occurred at the medium–to high-maturity stage, with a satisfactory hydrocarbon generation potential. Figure 4 shows that a very thick magmatic rock was developed in the Shanxi Formation in Well Cq16. The maturity of shale significantly increased within 75 m from the top and bottom of the magmatic rock, and no obvious abnormality was found in TOC and S_1+S_2. The shale of the Shanxi Formation and Taiyuan Formation in Well Jigu1 was not affected by magmatism, with R_o ranging from 0.75% to 1.02% (Chen et al., 2003; Yu et al., 2003). T_{max} of the shale of the Shanxi Formation in Well Lay1 ranged from 432.5°C to 477.5°C, the R_o value of the shale in the Taiyuan Formation ranged from 0.74% to 1.76%, and T_{max} ranged from 435.1°C to 475.8°C, mainly at the low-to medium-maturity stage.

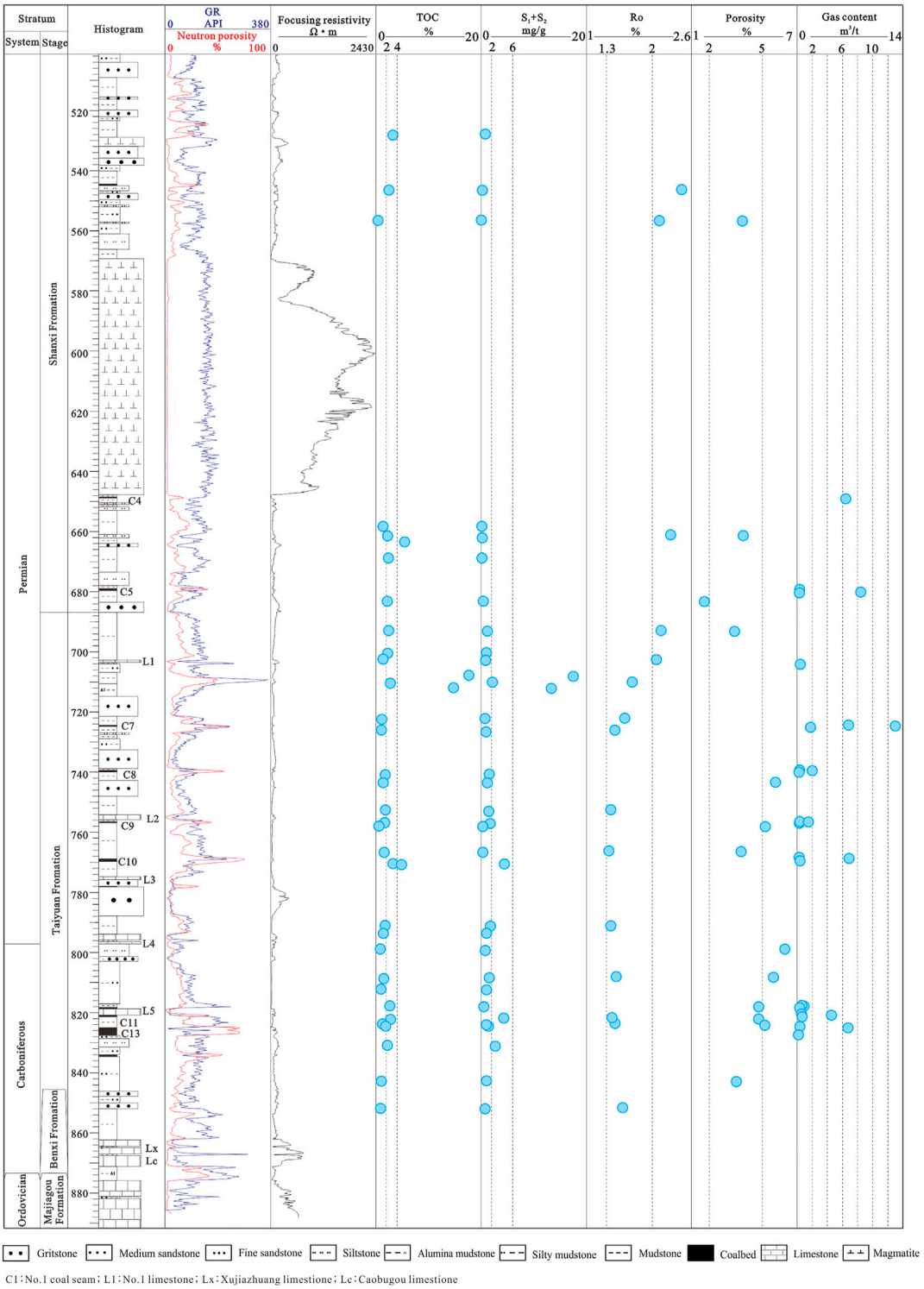

FIGURE 4
Geochemical and physical characteristics of the coal-measure source rock in Well Cq16.

Combined with the maximum reflectance data of shale vitrinite retrieved from the coalfield boreholes in the area, most shales of the Shanxi Formation and Taiyuan Formation in the whole study area occurred at the medium-mature stage and had entered the favorable area for SG generation. The organic matter maturity in the south was relatively low, mostly between 0.7% and 0.9%, followed by that in the east, while the maturity of the magmatic rock intrusion zone at the center was the highest.

4.2.3 Kerogen type

The sapropel, exinite, vitrinite, and inertinite contents in the coal seam of the Taiyuan Formation in adjacent Well Lay1 ranged

TABLE 2 Maceral content of shale in Wells Cq16 and Lay1.

Well number	Layer	Depth/m	Sapropelite/%	Exinite/%	Vitrinite/%	Inertinite/%	Type of organic matter
CQ16	Shanxi Formation	545.03	0	29	65	6	III
		660.51	0	60	22	18	III
	Taiyuan Formation	692.25	0	62	32	6	II2
		709.6	8	72	15	5	II2
		721.71	11	80	7	2	II1
		752.22	64	25	8	3	II1
		790.94	82	12	5	1	I
		807.88	90	5	4	1	I
		824.0	75	15	7	3	II1
		851.72	93	3	3	1	I
Lay1	Taiyuan Formation	1685.6	4	20	68	8	III
		1686.6	2	17	69	12	III
		1687.6	1	21	72	6	III
		1688.6	3	19	70	8	III
		1689.6	4	25	61	10	III
		1690.6	5	26	61	8	III
		1691.35	2	15	68	15	III
		1694.3	0	4	81	15	III
		1694.8	3	12	69	16	III
		1739.6	20	20	54	6	III
		1742.3	15	12	63	10	III
		1741.33	11	10	69	10	III
		1743.3	4	12	76	8	III
		1744.3	0	3	82	15	III
		1745.4	0	2	85	13	III

from 0% to 4%, 0% to 23%, 69% to 82% and 4% to 22%, respectively. The type of organic matter was Type III, which is consistent with the type of organic matter in the coal seam of the Taiyuan Formation in Well Liaogu2 (Hu et al., 2015). Since there are no measured data regarding the type of organic matter in the coal seams of the Shanxi Formation and Taiyuan Formation in the area, the type of organic matter in the coal seams in Wells Lay1 and Liaogu2 was determined to be Type III.

The sapropel content of shale in the Shanxi Formation in Well Cq16 reached 0, the exinite content ranged from 29% to 60%, the vitrinite content ranged from 22% to 65%, the inertinite content ranged from 6% to 18%, the TI value ranged from −40 to −5, and the organic matter type was Type III. The shale sapropel content in the Taiyuan Formation ranged from 0% to 93%, the exinite content ranged from 3% to 80%, the vitrinite content ranged from 3% to 32%, and the inertinite content ranged from 1% to 6% (Table 2). The organic matter type mainly included Type II, followed by Type I. The shale sapropel content in the Taiyuan Formation in Well Lay1 ranged from 0% to 20%, the exinite content ranged from 2% to 26%, the vitrinite content ranged from 54% to 85%, the inertinite content ranged from 6% to 16%, and the organic matter type was Type III.

4.3 Physical characteristics of the reservoir cap

4.3.1 Pore and fracture characteristics

The mercury injection porosity test results for the coal samples indicated that with increasing coal rank, the porosity of medium-rank coal seams first decreased from 4.29% to 2.72% and then increased to 4.56%, and the average porosity of the high-rank coal seams reached 5.38% (Meng, 2011). The pores of the coal reservoirs in the area were dominated by micropores (Meng, 2011). In Wells Zg18, Zg22 and Zg26, the permeability of each coal seam measured *via* the injection/pressure drop method exhibited a wide range and high heterogeneity. The permeability of the No. 7 coal seam ranged from 0.30 to 5.56 mD, that of the No. 10 coal seam was 0.53 mD, and that of the No. 13 coal

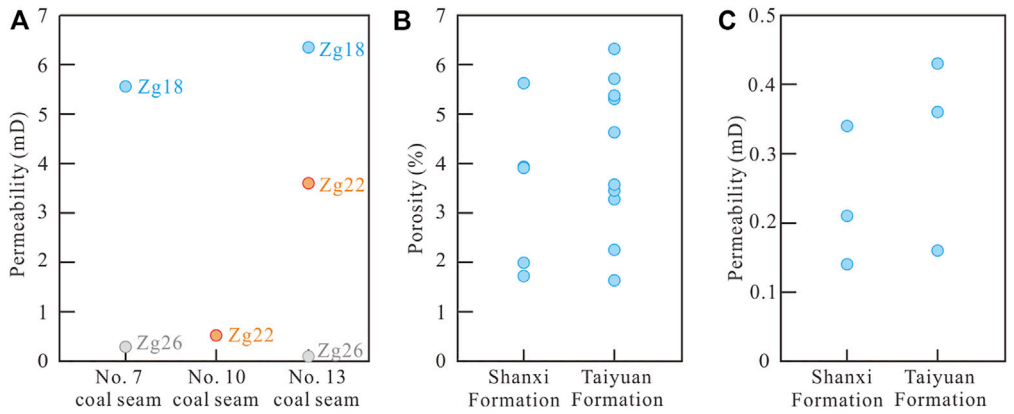

FIGURE 5
Permeability **(A)** of the No. 7, 10 and 13 coal seams in Wells Zg18, Zg22 and Zg26, and porosity **(B)** and permeability **(C)** of shale in the Shanxi Formation and Taiyuan Formation of Well Cq16.

seam ranged from 0.12 to 6.35 mD (Figure 5). In summary, the coal seams could be classified as a low-porosity and low-permeability reservoir.

The macrofractures in the coal reservoirs were more well developed than the microfractures. Fracture development was obviously affected by tectonic movement stress. The macrofractures could further connect several independently developed microfracture groups into a larger fracture system, thus generating an important seepage channel facilitating CBM diffusion, which more favorably affects the permeability of coal reservoirs. The microcracks are difficult to identify with the naked eye and can only be observed with a microscope or scanning electron microscope. The length of the microcracks is tens of microns to several millimeters, the height is hundreds of microns, and the width is on the scale of micrometers (Fu et al., 2007).

Microfractures were more developed in bright and semibright coal rock strata. The macroscale coal body structures of the No. 7, 10 and 13 coal seams mainly comprised primary and cataclastic structures. The macroscale coal rock types included semibright and semidark coal, with a largely moderate connectivity. Fractures were well developed. The main fractures ranged from 0.3 cm to 6.0 cm in length, the height ranged from 0.2 cm to 4.5 cm, the density ranged from 4 to 25 every 10 cm, and secondary fractures were not developed. The microscale coal rock type comprised semidark coal, with poor to moderate connectivity, slightly developed fractures and a slight overall fracture density difference, among which the No. 10 coal seam contained the most well-developed fractures (Table 3). The microscopic type in the area exhibited a crack width of >5 μm, and fractures with a length of 10 mm≥L≥1 mm constituted the main part. Compared to the Ordos Basin, Qinshui Basin and Lianghuai Coalfields in the North China Craton (Yao, 2006; 2007; Hu, 2016; Zhang, 2017), the width and length of the microfractures in the Huanghebei Coalfield were larger, but the spatial density was slightly lower.

The porosity of the shale of the Shanxi Formation in Well Cq16 ranged from 1.73% to 5.63%, and the permeability ranged from 0.14 to 0.34 mD (Figure 5). The porosity of the shale of the Taiyuan Formation ranged from 1.63% to 6.32%, and the shale permeability ranged from 0.16 to 0.43 mD (Figure 5). The shale of the Taiyuan Formation and Shanxi Formation revealed similar porosity and permeability conditions, both belonging to low-porosity and low-permeability reservoirs.

4.3.2 Mechanical properties

Rocks with a high elastic modulus and low Poisson's ratio are relatively more brittle and are more likely to form natural and pressure-induced fractures (Yan et al., 2015). The compressive strength of rocks with natural fractures is lower (Miao et al., 2021). The rock mechanical property test results of Wells Zg18, Zg22, Zg26 and Cq16 indicated that the elastic modulus of the shale of the Shanxi Formation was 9.6 GPa, Poisson's ratio was 0.18. Moreover, the elastic modulus of the shale of the Taiyuan Formation ranged from 6.7 to 18.3 GPa, with an average of 10.19 GPa, and Poisson's ratio ranged from 0.09 to 0.19, with an average of 0.15. The elastic modulus and Poisson's ratio of the shale above were lower than those of the Bakken, Marcellus, Woodford, Eagle Ford, Haynesville, Barnett, Jiaoshiba and other typical SG reservoirs in China and elsewhere (Sheng et al., 2016). The tensile strength of the shale of the Shanxi Formation in Wells Zg18, Zg22, Zg26 and Cq16 was 2.51 MPa, and the compressive strength reached 32.1 MPa. The tensile strength of the shale of the Taiyuan Formation ranged from 0.66 to 5.13 MPa, with an average of 1.61 MPa, and the compressive strength ranged from 12.6 to 74.9 MPa, with an average of 31.08 MPa (Figure 6). The tensile and compressive strengths of the shale were low. The above mechanical parameters comprehensively indicate that the shale in this area exhibited favorable fracturing properties.

4.4 Gas occurrence trend and gas-bearing characteristics

The Langmuir volume (V_L) represents the maximum adsorption capacity of the reservoir, and the Langmuir pressure (P_L) reflects the difficulty of reservoir analysis (Fu, 2007). The isothermal adsorption

10.3389/feart.2023.1104418

TABLE 3 Microfracture characteristics of the coal seams in the Huanghebei Coalfield.

Coal seam	Coal petrographic type	Connectivity	Fracture development degree	Main fissure				Secondary fissure			
				Length (cm) min-max/average	Height (cm) min-max/average	Width (μm) min-max/average	Density (strip/10 cm)	Length (cm) min-max/average	Height (cm) min-max/average	Width (μm) min-max/average	Density (strip/10 cm)
7	Semidark coal	Poor-Medium	Relatively developed	0.01–3.3/0.54	0.04–1.5/0.44	1–90/11	28	0.04–0.8/0.21	0.03–0.6/0.21	1–20/7	1.2
10	Semidark coal	Medium	Developed	0.005–1.2/0.28	0.005–1.2/0.22	1–50/10	84	0.005–0.5/0.09	0.005–0.8/0.16	1–30/6	5.4
13	Semidark coal	Poor-Medium	Relatively developed	0.01–1.8/0.33	0.01–2.3/0.51	1–40/8	21–39	0.01–2.1/0.33	0.005–1.3/0.32	1–40/7	1.3–3.2

test results for the coal seams in the southern part of the study area demonstrate (Table 4) that the V_L of the No. 7 and 10 coal seams was large, indicating a high adsorption capacity, while the adsorption capacity of the No. 11 and 13 coal seams subjected to magmatic erosion was lower. The P_L values of the No. 11 and 13 coal seams were higher than those of the No. 7 and 10 coal seams, and desorption was relatively difficult. The coal reservoir pressure increased with increasing burial depth, among which the maximum pressure of the No. 13 coal seam reached 7.04 MPa, while the pressure gradient and gas saturation parameters of the No. 7, 10 and 13 coal seams generally indicated underpressurized and undersaturated reservoirs, respectively.

The total gas contents in the No. 5, 7 and 10 coal seams were higher than those in the No. 11 and 13 coal seams, which was mainly caused by the notable escape of coal seam gas from the No. 11 and 13 coal seams due to lower magmatic rock intrusion. The molecular diameter of N_2 is small, which easily diffuses and migrates over a long distance and gradually becomes enriched along the direction of CMG transport (Shen et al., 2021). CBM in the No. 5, 7 and 10 coal seams in the study area was dominated by CH_4, followed by N_2, while the CBM occurring in the No. 4, 11 and 13 coal seams was dominated by N_2, followed by CH_4, which confirms that CBM near magmatic rocks had migrated throughout the transport system.

The measured data of the SG content were all retrieved from Well Cq16. The gas content in the two shale samples of the Shanxi Formation ranged from 0.25 to 0.34 m^3/t, with an average of 0.30 m^3/t. The gas content in the 14 shale samples of the Taiyuan Formation ranged from 0.17 to 6.80 m^3/t, with an average of 0.93 m^3/t. According to the gas logging data of Wells Zg18, Zg22 and Zg26, gas logging anomalies were observed in the shale section, fine sandstone section, limestone section and a small range of the magmatic rock section between the No. 5 coal seam and No. 13 coal seam floor; notably, SG, TG, carbonate rock gas and magmatic rock gas occurred, respectively. The measured data of SG in the study area were relatively limited, but a large amount of TOC data was available. Because the TOC content is positively correlated with the gas content (Zou et al., 2014), a linear relationship model (Li et al., 2021) could be established between the SG and TOC contents in the Luxi uplift area (Figure 7), and the SG content in the area was thus estimated to vary between 0.25 and 0.53 m^3/t according to the TOC content.

4.5 Creation of several independent gas-bearing systems by the key gas barrier

The coal-measure hydrocarbon source rock exhibited a moderate organic matter abundance, satisfactory hydrocarbon generation potential and wide-covering sedimentary characteristics. The source rock was mainly developed in the TST and HST of sequence SIII2 and the TST of sequence SIII3. The source rock comprised a lagoon tidal flat and lower delta plain deposit. The CMG reservoir forming characteristics, such as source reservoir dependency, reservoir cap interaction, and multiple seals, yield a complex gas–water distribution relationship in coal measures, and multifluid pressurized systems are often developed vertically (Yang et al., 2021). Figure 2 shows that each gas-bearing interval was stably developed. There occurred lagoon facies of the Taiyuan Formation and thick fine sediments of the interdistributary bay of the Shanxi Formation between the intervals, which could be regarded as regional cap rocks and were

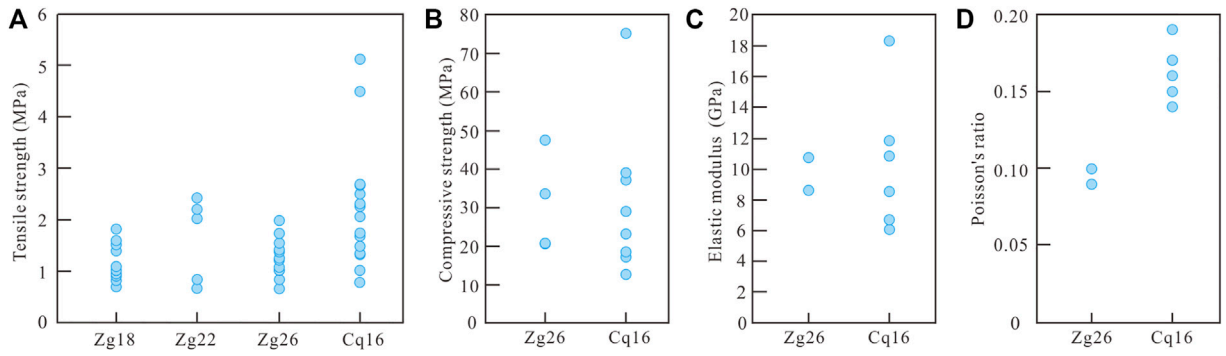

FIGURE 6
Mechanical parameters of shale rock in the Taiyuan Formation of Wells Zg18, Zg22, Zg26 and Cq16, including tensile strength **(A)**, compressive strength **(B)**, elastic modulus **(C)** and Poisson's ratio **(D)**.

relatively independent gas-bearing units. The siderite mudstone layer was characterized by a low porosity and permeability and high breakthrough pressure. As a key layer of water and gas resistance developed near the most extensive flooding surface, it formed the boundary of the coal series superimposed gas-bearing system (Shen et al., 2017). The main Carboniferous-Permian SG layers in western Shandong generally contain siderite (Zhang et al., 2020). The distribution of the siderite mudstone layer plays an important role in the development of independent gas-bearing units.

The discovery of carbonate gas indicates that the marine limestone marker bed is a reservoir rather than a gas barrier. Due to the influence of multistage transgression, for example, coal-measure limestone can develop into a suitable reservoir with many fractures/fractures or even karst caves, which can form a carbonate gas reservoir after receiving external CMG (Fu, 2018; Shi et al., 2020). The Taiyuan Formation in this area contains multiple well-developed marine marker beds with well-developed fractures and a certain gas storage space. The gas logging data for Wells Zg18, Zg22 and Zg26 indicated gas logging anomalies in the L2, L3 and L5 limestone marker beds, which were mainly caused by the migration of received near-source CMG.

The Ordos Basin and Bohai Bay Basin generally develop weathering crust karst reservoir paleogeomorphic gas reservoirs atop the Ordovician System, forming a reservoir cap combined with the bauxite mudstone of the Benxi Formation (Liang et al., 2016; Chi et al., 2021). There are many cases of high-angle normal faults cutting the Ordovician limestone roof in the study area. Against the structural background of the regional gentle monocline and NW-trending stepped normal faults, deep CMG migrates vertically and laterally along the fault to the top of the Ordovician to form near-source gas reservoirs. The sandstone reservoirs in the study area mainly include tidal flat facies sand bodies of the Taiyuan Formation, distributary channel sand bodies of the Shanxi Formation and fluvial facies of the Shihezi Formation. The sand bodies exhibited favorable physical properties and high heterogeneity. They were superimposed and inlaid in the coal measures during many periods. The vertical thickness was large, and they provided the basis for the development of large areas of multilayer high-quality reservoirs. Under the condition of satisfactory wall rock capping, coal measures are mostly developed in low-abundance gas field areas with notable small-scale segmentation and a large number of gas reservoirs (Li et al., 2021). At present, only shallow tight sandstone gas has been found in the Taiyuan Formation in the southern part of the study area. It is believed that with the further development of deep exploration in the north, CMG originating from magmatic rocks, fault systems, microfractures and hydrodynamic transport systems can be found in the sand bodies of the Shanxi Formation and Shihezi Formation. Therefore, the deep Ordovician top boundary weathering crust, Shanxi Formation and Shihezi Formation sand bodies in the study area should be the focus of CMG exploration in this area.

4.6 Types of CMG reservoirs

The types of CMG reservoirs can be divided into unconventional continuous-type (source coalbed gas, source SG and near-source TG) and conventional trap-type reservoirs (Zou et al., 2019). Gas reservoirs often repeatedly overlap, and there are multiple types of gas reservoir combinations (Zhu et al., 2016). At present, Carboniferous–Permian CMG reservoirs are found in the southern part of the study area and are mainly near-source and source reservoirs. Due to the relatively large burial depth of the main hydrocarbon source rocks in the northern part of the study area, no targeted drilling has been performed. However, according to the current geological understanding, it is believed that there exists a higher possibility of remote source gas reservoirs or conventional trap-type gas reservoirs in the north. Coal seams are prone to vertical migration due to the presence of numerous developed vertical fractures. Moreover, shale fractures are not developed, the bedding direction permeability is obviously higher than the vertical direction permeability, and lateral migration easily occurs. CMG mainly undergoes rapid overpressure flow migration driven by hydrocarbon generation pressurization and molecular diffusion flow migration driven by the hydrocarbon concentration gradient under the effect of the residual pressure difference with the source reservoir.

According to the spatial combination type of source, reservoir and cap rock, the CMG reservoirs in the Huanghebei Coalfield can be divided into three types (Figure 8), namely, heterogeneous gas reservoirs, self-sourced gas reservoirs and self-sourced+heterogeneous near-source superimposed gas reservoirs. The Shanxi Formation mainly contains SG reservoirs, namely, self-sourced gas reservoirs. There are many types of gas reservoir combinations in the Taiyuan Formation, including coalbed gas, SG,

TABLE 4 Analysis results of the CBM content in each coal seam.

Coal seam	Total gas content (m^3/t)	CH_4 concentration (m^3/t)	Gas composition (%)			Langmuir volume (m^3/t)		Langmuir pressure (MPa)	Reservoir pressure (MPa)	Pressure gradient (MPa/100 m)	Gas saturation (%)	Permeability (mD)	R_o (%)
			CH_4	CO_2	N_2	Air dried basis	Dry ash free base						
4	6.44 (1)	1.24 (1)	21.73 (1)	0.15 (1)	73.46 (1)	—	—	—	—	—	—	—	—
5	8.42 (1)	3.84 (1)	58.20 (1)	6.65 (1)	33.30 (1)	—	—	—	—	—	—		0.78–2.26/1.08 (6)
7	0.32–12.99/6.32 (8)	0.23–10.55/5.05 (8)	5.47–95.68/56.13 (8)	0.58–10.03/3.84 (8)	1.05–90.70/39.88 (8)	24.81–28.22/26.21 (3)	34.93–37.40/36.11 (3)	3.26–3.51/3.34 (3)	0.49–5.52/3.00 (2)	0.10–0.97/0.54 (2)	26–73	0.30–5.56/2.93 (2)	0.66–3.72/1.28 (38)
10	0.35–16.54/6.76 (10)	0.12–16.29/5.77 (10)	9.86–98.58/63.15 (10)	0.40–16.66/4.20 (10)	0.40–73.48/32.53 (10)	29.46–30.57/30.02 (2)	37.12–38.17/37.65 (2)	3.04–3.40/3.22 (2)	4.20 (1)	0.80 (1)	59	0.53 (1)	0.61–4.52/1.51 (42)
11	0.35–4.55/2.01 (3)	0.11–1.09/0.54 (3)	32.82–39.92/36.57 (3)	0.47–4.23/2.44 (3)	54.00–66.70/59.83 (3)	19.09 (1)	21.94 (1)	5.92 (1)	—	—	—	—	0.62–6.35/2.22 (69)
13	0.13–6.73/1.78 (11)	0.03–3.66/1.19 (11)	0.64–76.07/35.28 (11)	0.16–16.20/6.18 (11)	4.90–96.48/55.21 (11)	25.19–29.33/26.97 (2)	32.13–40.87/36.05 (2)	4.03–4.21/4.13 (2)	6.02–7.04/6.46 (3)	0.85–0.93/0.89 (2)	1–4	0.12–6.35/3.36 (3)	0.62–5.87/1.49 (117)

CBM, content analysis was conducted for Well Cq16 at the No. 4, 5, 7, 10, 11 and 13 coal seams, for Well Zg18 at the No. 7, 10 and 13 coal seams, for Well Zg22 at the No. 7, 10 and 11 coal seams, and for Well Zg26 at the No. 7, 10, 11 and 13 coal seams. Isothermal adsorption tests were carried out for nine layers of coal in Wells Zg18, Zg22 and Zg26, and injection/pressure drop tests were carried out for six layers of coal. In addition, the following data were obtained from the previous exploration report: six vitrinite reflectance values for the No. 5 coal seam, 4 gas contents and 35 vitrinite reflectance values for the No. 7 coal seam, 6 gas contents and 40 vitrinite reflectance values for the No. 10 coal seam, 68 vitrinite reflectance values for the No. 11 coal seam, and 8 gas contents and 114 vitrinite reflectance values for the No. 13 coal seam. Similar data structure 0.32-12.99/6.32 (8) represented min-max/average (number of data).

10.3389/feart.2023.1104418

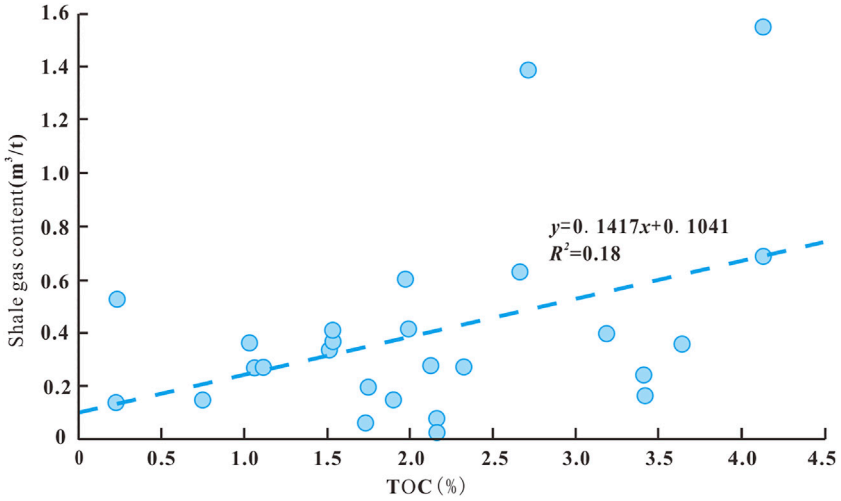

FIGURE 7
Linear relationship between the SG and TOC contents in the western Shandong coal-bearing area Li et al., 2021.

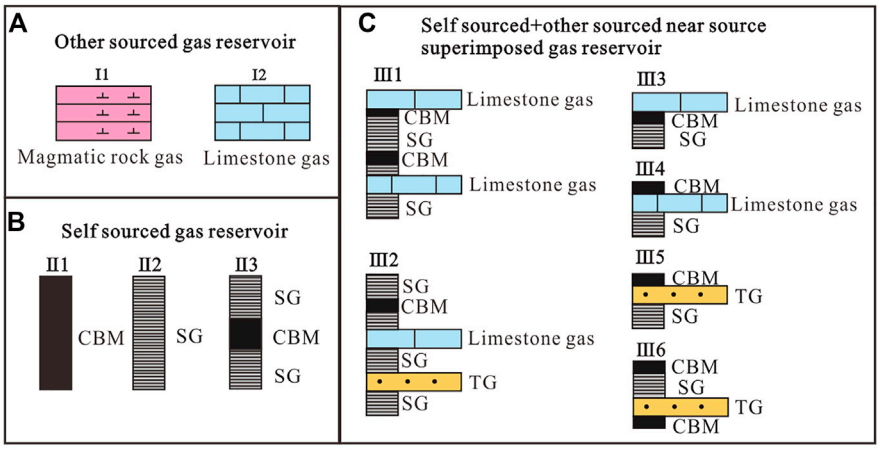

FIGURE 8
Three types of CMG reservoirs, namely, other-source gas reservoirs **(A)**, self-sourced gas reservoirs **(B)** and self-sourced+other-source near-source superimposed gas reservoirs **(C)**.

tight sandstone gas, carbonate rock gas and magmatic rock gas reservoirs. Self-sourced gas reservoirs and self-sourced+other-source near-source gas reservoirs dominate, followed by other-source gas reservoirs. Among them, self-sourced gas reservoirs and self-sourced+other-source near-source gas reservoirs exhibit the highest gas content and the most obvious gas logging anomalies.

(1) Type I: Other-source gas reservoir.

This type of gas reservoir contains independent magmatic rock gas and carbonate rock gas units (I1-I2), which is mainly a fracture-type reservoir, and the gas source encompasses near-source coalbed gas and SG. Deep natural gas vertically and laterally migrated and accumulated in the fractures of limestone and magmatic rock and was sealed by the overlying thick fine sediment for preservation. The abnormal section of limestone gas logging was obviously wider than that of magmatic rock, indicating that the reservoir space was more notably developed.

(2) Type II: Self-sourced gas reservoir.

This type of gas reservoir mainly exists independently or in combination with CBM and SG reservoirs and can be divided into three combinations (II1-II3). In combination II3, CBM mainly migrates vertically into the SG reservoir, and the overall gas content gradually decreases from the center of the coal seam toward the shale at the top and bottom.

(3) Type III: Self-sourced + other-source near-source superimposed gas reservoir.

CBM, SG, TG and carbonate rock gas reservoirs overlap, and there are six combinations (III1-III6). CBM mainly play the role of vertical interbed migration paths, supplying gas to adjacent limestone and tight sandstone reservoirs. SG is mainly transported along transverse layers to balance the gas energy.

Figure 2 shows that when the roof and floor of the coal seam solely comprise shale or silty mudstone, the overpressure peak pointing

TABLE 5 Overview of CBM resources.

Coal seam	Medium-rank CBM (10^8 m^3)	High-rank CBM (10^8 m^3)	Total (10^8 m^3)
5	36.19	6.70	42.89
7	39.48	5.67	45.15
10	34.08	4.76	38.84
13	6.82	4.19	11.01
Total	116.57	21.32	137.89

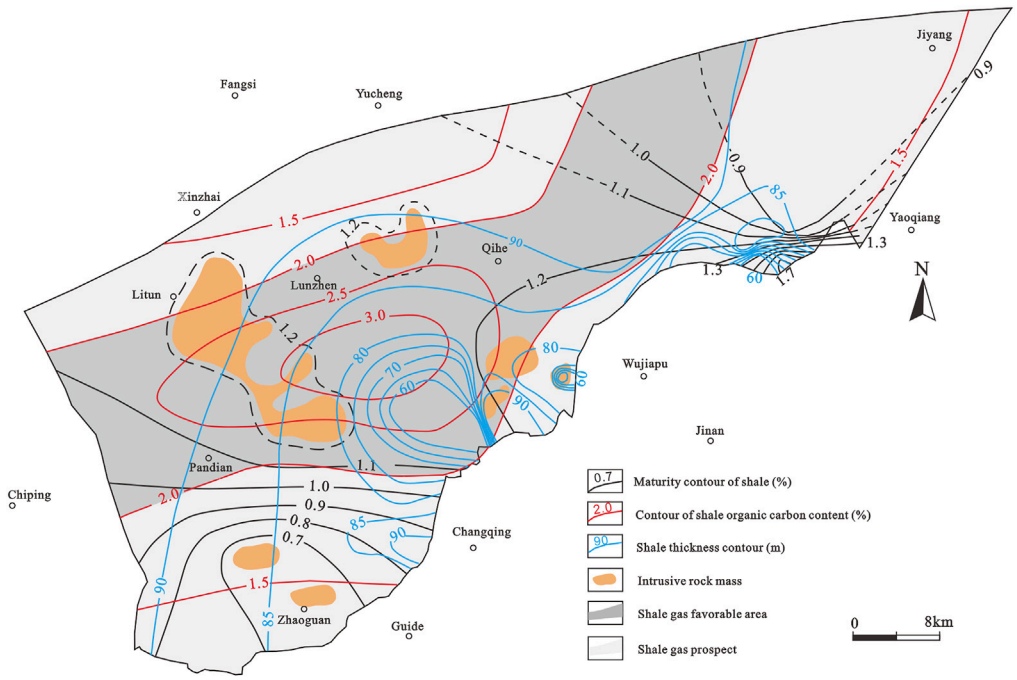

FIGURE 9
Distribution of shale thickness, TOC, maturity and favorable areas in the Shanxi Formation and Taiyuan Formation.

TABLE 6 Reference standard for SG area selection in the Huanghebei Coalfield.

Constituency	Thickness of the shale series	TOC (%)	Ro (%)	Burial depth (m)	Surface conditions	Preservation conditions	Magmatic rock development
Favorable area	Ratio of the effective shale series to the stratum thickness: >60%; the thickness of a single layer mudstone: >6 m; and the continuous thickness: ≥30 m	Average not less than 2.0%	Type II kerogen ≥0.9%; Type III kerogen ≥0.7%	500 ~ 4500	Preferably	Medium structure, continuous stratigraphic development, and a traceable correlation	Close to the target stratum series, without intruding into the effective rock stratum
Prospective area	No requirement	Average not less than 0.5%	Not less than 0.4%	100 ~ 4500	Preferably	There is development and a certain distribution of regional shale series, with general preservation conditions	No requirement

phenomenon easily occurs, such as in the II3 and III2 combinations. The reason is that when the coal seam and shale function as cap rocks, the hydrocarbon generation capacity of the coal seam is better than that of shale, which plays a role in inhibiting and preventing the escape of shale hydrocarbons, and the shale sealing capacity is notable. Self-generated gas can mitigate the concentration sealing effect of CBM

migration (Zhu et al., 2016). When the top or bottom of the coal seam comprises limestone, the limestone provides poor porosity and permeability conditions, but fissures are relatively well developed, CBM escapes into the limestone under the sealing effect of mudstone, and the peak amplitude of the coal seam is reduced to a certain extent. The shale limits the gas escape process due to the high hydrocarbon generation intensity of the coal seam, such as the III1, III3, and III4 combinations. When the roof of the coal seam comprises argillaceous shale or silty mudstone and the floor comprises fine sandstone, as CBM can diffuse along the underlying stratum through fine sandstone with relatively favorable porosity and permeability conditions, the amplitude of the CBM peak is reduced to a certain extent, such as the III5 combination. When the roof of the coal seam comprises fine sandstone, due to the poor sealing conditions of the fine sandstone, the peak pointing phenomenon of CBM is not obvious. For example, in combination III6, CBM at the bottom escapes into the fine sandstone to form tight sandstone gas. At the same time, CBM enters the overlying shale and coalbed through the fine sandstone migration medium, thus enhancing the peak pointing phenomenon of overpressure in the upper coal seam. In general, the interbedded combination of coal seams and shale is the most conducive to CMG preservation, and the overall gas content is high.

5 Resources and evaluation of the CMG accumulation system

The No. 5, 7, 10 and 13 coal seams are the main CBM reservoirs in this area and are also the target reservoirs in this paper. According to the regulation of coalbed methane reserve estimation (DZ/T 0216-2020), the methods for estimating CBM resources are the volume method and analogy method. The volume method is the basic method for estimating the geological reserves of CBM, which is applicable to the calculation of CBM reserves at all levels. Its accuracy depends on the understanding of the extent of block exploration, geological conditions and reservoir conditions. The analogy method is mainly based on comparison of the geological parameters and engineering parameters of the developed CBM fields or adjacent CBM fields and is often used when the exploration degree of the block is low. Therefore, the volume method is used to estimate the CBM resource quantity. The estimation formula is

$$G_i = 0.01AhDC_{ad} \quad (1)$$

where G_i is the geological reserves of coalbed methane, 10^8 m^3; A is the coal seam gas bearing area, km^2; h is the net thickness of the coal seam, m; D is the apparent density of coal on an air-dried basis, t/m^3; and C_{ad} is the air content of coal on an air-dried basis, m^3/t.

The shallow area with an elevation of −500 m belongs to the wind oxidation zone, and the resource quantity is thus not estimated. Based on the data of 569 coalfield boreholes and 4 CBM boreholes in 20 exploration areas within the Huanghebei Coalfield and relevant test data, the CBM resource quantity at an elevation ranging from approximately −500 to −2000 m was evaluated using the volume method (Table 5). The estimated area was 2267 km^2, the initial thickness of the coal seam was 0.50 m, and the initial standard of the CBM content was 1 m^3/t (air-dried basis). The CBM resources of the No. 5, 7, 10 and 13 coal seams amounted to 42.89 × 10^8 m^3, 45.15 × 10^8 m^3, 38.84 × 10^8 m^3 and 11.01 × 10^8 m^3, respectively, with total resources of 137.89 × 10^8 m^3. Among them, the resource amount of medium-rank CBM was 116.57 × 10^8 m^3, and the high-rank CBM resource amount reached 21.32 × 10^8 m^3.

To reflect the current situation of SG resource exploration in the study area more accurately, based on Zhang et al.'s (2012) optimal conditions for favorable and prospective areas of SG in China, the criteria for the selection of favorable areas were adjusted according to the control degree in this SG survey. Please refer to Table 6 for specific criteria for area selection. As such, favorable and prospective areas for the development of SG resources in the Carboniferous–Permian system could be identified in the Huanghebei Coalfield (Figure 9). According to the standard for shale gas resources and reserves estimation (DZ/T 0254-2020), the analogy method, volumetric method and volumetric method can be used for shale gas resource estimation. Different from the other two methods, the analogy method is applicable to the estimation unit without measured gas content and gas saturation data. If the shale section does not contain crude oil, the volume method can be used to estimate the total shale gas resources.

$$Q = 0.01A_g h\rho_y C_Z \quad (2)$$

where Q is the total resources, 10^8 m^3; A_g is the gas bearing area, km^2; h is the effective thickness, m; ρ_y is the shale mass density, t/m^3; and C_z is the total gas content in the shale interval, m^3/t.

Since the measured total shale gas content in the area is limited, the total shale gas content in each block can be estimated using TOC data through the linear relationship model of shale gas content and TOC content (Figure 7). The total amount of SG resources was estimated at 2100.45×10^8 m^3 *via* the volumetric method. Among them, the resource amount in the favorable area reached 1075.77×10^8 m^3, with a resource amount of 1024.68×10^8 m^3 in the prospective area.

6 Conclusion

Based on source reservoir geochemical characteristics, reservoir cap physical properties and gas-bearing properties, the reservoir-forming effect of the CMG accumulation system in the Huanghebei Coalfield was analyzed, and the potential of CMG resources was evaluated. The following three main conclusions could be obtained:

(1) The CMG source rocks mainly included the shale and coal seams of the Taiyuan Formation and Shanxi Formation, providing a favorable material basis for CMG enrichment. The coal seams were mainly mature to highly mature coal seams, with a satisfactory hydrocarbon generation potential. They belonged to low-porosity, low-permeability, underpressurized and undersaturated reservoirs. The N_2 content among the CBM components greatly affected by faults, magma and other transport systems exceeded the CH_4 content. The shale organic matter was mainly Type II, with a moderate organic matter abundance. The material reached the middle-to high-maturity stage, provided satisfactory hydrocarbon generation potential, belonged to a low-porosity and low-permeability reservoir, and exhibited favorable fracturing properties.

(2) As regional caprocks, the thick fine sediments of the lagoon facies of the Taiyuan Formation and the interdistributary bay of the Shanxi Formation, combined with the sideritic mudstone of the

key gas barrier, created several stable and independent gas-bearing systems. The combination types of CMG reservoirs mainly included self-sourced gas reservoirs and self-sourced+heterogeneous near-source gas reservoirs, followed by heterogeneous gas reservoirs. CBM and SG play vertical and horizontal regulatory roles, respectively. Sand bodies, magmatic rocks, fault systems, microfractures and hydrodynamic forces, as macroscale transport systems, expand the development space of heterogeneous gas reservoirs.

(3) CMG in the Huanghebei Coalfield mainly includes SG, coalbed gas and a small amount of tight sandstone gas, carbonate rock gas and magmatic rock gas. The SG and CBM resources are abundant, and the CBM resource amount is $137.89 \times 10^8\ m^3$, while the coal SG resource amount reaches $2100.45 \times 10^8\ m^3$.

Data availability statement

The original contributions presented in the study are included in the article/supplementary material, further inquiries can be directed to the corresponding authors.

Author contributions

YSH and YG: Contributed equally to this research. YSH, XH, YW, SZ, YZ, and LS: Field investigation. XH, YSO, MW, KC, and QY: Data analysis. YSO: Writing—original draft preparation. YSO, HW, YG, and XH: Writing—review and editing. All authors listed have made substantial, direct, and intellectual contributions to the work and approved it for publication.

Funding

This study was carried out in the financial support of the 2022-2023 key scientific research project of Shandong Coalfield Geology Bureau (2022-17, 2022-18 and 2022-55), Natural Science Foundation of Shandong Province (ZR2020MD031), and the special fund project of geological exploration in Shandong Province Exploration Prospect (2013-6 and 2013-144). We thank our scientific research team for their help and guidance in the field investigation.

Conflict of interest

The authors declare that the research was conducted in the absence of any commercial or financial relationships that could be construed as a potential conflict of interest.

Publisher's note

All claims expressed in this article are solely those of the authors and do not necessarily represent those of their affiliated organizations, or those of the publisher, the editors and the reviewers. Any product that may be evaluated in this article, or claim that may be made by its manufacturer, is not guaranteed or endorsed by the publisher.

References

Bi, C. Q., Hu, Z. F., Tang, D. Z., Tao, S., Zhang, J. Q., Tang, S. L., et al. (2021). Research progress of coal-measure gas and some important scientific problems. *Geol. China* 48 (2), 402–423. (in Chinese with English Abstract). doi:10.12029/gc20210205

Bi, C. Q., Zhang, J. Q., Shan, Y. S., Hu, Z. F., Wang, F. G., Chi, H. P., et al. (2020). Geological characteristics and co-exploration and co-production methods of Upper Permian Longtan coal measure gas in Yangmeishu syncline, Western Guizhou Province, China. *China Geol.* 3 (1), 38–51. doi:10.31035/cg2020020

Cao, D. Y., Yao, Z., and Li, J. (2014). Evaluation status and development trend of unconventional gas in coal measure. *Coal Sci. Technol.* 42 (1), 89–105. (in Chinese with English Abstract). doi:10.13199/j.cnki.cst.2014.01.021

Chen, Y. H., Lin, Y. X., and Jiang, H. C. (2003). The potential of gas generation from coal bearing formation in Huimin Sag. *Coal Geol. Explor.* 31 (03), 26–29. (in Chinese with English Abstract).

Chi, X. Q., Feng, Q. H., Xu, S. M., and Shu, P. (2021). Facies control of weathering crust reservoir in mawu1-4 sub-members of Ordos Basin: Case study of tao 2 block in sulige gas field. *Nat. Gas. Geosci.* 32 (09), 1358–1371. (in Chinese with English Abstract). doi:10.11764/j.issn.1672-1926.2021.03.013

Clarkson, C. R. (2013). Production data analysis of unconventional gas wells: Workflow. *Int. J. Coal Geol.* 109-110, 147–157. doi:10.1016/j.coal.2012.11.016

Cui, X. C. (2004). *Evaluating on coal gas source rock of Carboniferous-Permian in Huanghebei coalfield and Jiyang basin*. Qingdao: Shandong University of Science and Technology. (in Chinese with English Abstract).

Dai, J. X., and Gong, J. M. (2018). Establishment of coal-derived gas geological theory and its strategic significance to the development of natural gas industry in China. *China Pet. Explor.* 23 (04), 1–10. (in Chinese with English Abstract). doi:10.3969/j.issn.1672-7703.2018.04.001

Fan, S. Y., Wu, X. R., and Guo, J. P. (2001). Evaluation of coal gas resource in Huanghebei coal field, Shandong Province. *Geol. China* 28 (6), 28–30. (in Chinese with English Abstract). doi:10.3969/j.issn.1000-3657.2001.06.005

Fu, X. H., Chen, Z. S., Song, R., and Zhang, Q. H. (2018). Discovery of coal measures limestone gas and its significance. *Coal Geol. China* 30 (06), 59–63. (in Chinese with English Abstract). doi:10.3969/j.issn.1674-1803.2018.06.12

Fu, X. H., Ge, Y. Y., Liang, W. Q., and Li, S. (2013). Pressure control and fluid effect of progressive drainage of multiple superposed CBM systems. *Nat. Gas. Ind.* 33 (11), 35–39. (in Chinese with English Abstract). doi:10.3787/j.issn.1000-0976.2013.11.006

Fu, X. H., Qin, Y., and Wei, C. T. (2007). *Coalbed gas geology*. Xuzhou: China University of Mining and Technology Press. (in Chinese with English Abstract).

He, R. W., Du, Y. M., Liu, J., and Liu, Y. L. (2005). Gas generation model of Permo-Carboniferous coal in south slope of Huimin Sag. *Coal Geol. Explor.* 33 (4), 42–44. (in Chinese with English Abstract). doi:10.3969/j.issn.1001-1986.2005.04.011

Hou, X. W., Zhu, Y. M., and Yao, H. P. (2018). Coupled accumulation characteristics of Carboniferous-Permian coal measure gases in the Northern Ordos Basin, China. *Arab. J. Geosci.* 11, 156–169. doi:10.1007/s12517-018-3512-8

Hu, X. C., Zhou, Y. Q., and Zhang, F. X. (2015). The characteristics of coal source rock in Taiyuan Formation of eastern linqing depression and its main controlling factors. *Sci. Technol. Eng.* 15 (06), 41–47. (in Chinese with English Abstract).

Hu, Z. Z., Huang, W. H., Liu, S. P., Zhang, Q., Xu, Q. L., and Feng, X. L. (2016). Study on the influencing factors of the microfracture development in coal reservoir in southern Qinshui basin. *Coal Geol. Explor.* 44 (05), 63–70. (in Chinese with English Abstract).

Huang, D. F., and Xiong, C. W. (1996). Generation, migration and evaluation of hydrocarbon generation potential of oil formed in coal-bearing strata. *Explorationist* 1 (2), 6–11. (in Chinese with English Abstract).

Huang, X. L. (2018). Study on occurrence characteristics and controlling factors of coalbed methane in Zhaoguan Coalfield. *Coal Sci. Technol.* 46 (4), 196–201. (in Chinese with English Abstract). doi:10.13199/j.cnki.cst.2018.04.031

Huang, X. L., Zhong, J. W., and Xu, Y. G. (2012). Two tales of the continental lithospheric mantle prior to the destruction of the North China Craton: Insights from Early Cretaceous mafic intrusions in Western Shandong, East China. *Geochimica Cosmochimica Acta* 96, 193–214. doi:10.1016/j.gca.2012.08.014

Jia, Q., and Lv, D. W. (2009). Sequence division and eustatic area level change of Carberours-Permian systems in Liaocheng, Shandong Province. *North West. Geol.* 42 (2), 108–115. (in Chinese with English Abstract).

Jin, Q., Song, G. Q., Liang, H. B., Cheng, F. Q., and Wang, L. (2009). Characteristics of carboniferous -permian coal-derived gas in the Bohai Bay Basin and their implication to exploration potential. *Acta Geol. Sin.* 83 (06), 861–867. (in Chinese with English Abstract).

Law, B. E., and Curtis, J. B. (2002). Introduction to unconventional petroleum systems. *AAPG Am. Assoc. Pet. Geol.) Bull.* 86, 1851–1852. doi:10.1306/61eedda0-173e-11d7-8645000102c1865d

Li, C. F., Huang, X. L., Shao, Y. B., and Dou, F. K. (2021). Shale gas exploration potential in southwestern Shandong Province of eastern China. *Front. Earth Sci.* 9, 1–17. doi:10.3389/feart.2021.702902

Li, G., Yang, Z. B., Gao, W., Zhang, Z. G., Jiang, B. R., and Lu, B. J. (2022). Characteristics of coal-measure gas reservoirs in thin interbedded marine–continental transitional facies and optimization of combined production: Examples from the tucheng syncline in western Guizhou. *Nat. Resour. Res.* 31 (3), 1503–1522. doi:10.1007/s11053-022-10053-8

Li, J. T., Li, Z. X., Yu, J. F., Guo, J. B., Liu, X. L., and Liu, H. F. (2022). Stratigraphic sequence correlation based on wavelet transform of well - logging data: Taking the coal-bearing strata of permian - carboniferous system in Luxi and jiyang area as an example. *Acta sedimentol. sin.* 23 (4), 639–645. (in Chinese with English Abstract).

Li, Y. G. (2019). Research on coalbed methane geological characteristics and exploration direction of No.7 coal seam in Huanghebei coalfield. *China Coalbed Methane* 16 (5), 2441. (in Chinese with English Abstract).

Li, Y., Xu, W. K., Gao, J. X., Wu, P., Tao, C. Q., Tian, Y., et al. (2021). Mechanism of coal-measure gas accumulation under integrated control of "source reservoir-transport system": A case study from east margin of Ordos Basin. *J. China Coal Soc.* 46 (08), 2440–2453. (in Chinese with English Abstract). doi:10.13225/j.cnki.jccs.CB21.0765

Li, Z. (2006). Hydrocarbon-generation evolution of permian-carboniferous source rock in jiyang depression. *Acta Pet. Sin.* 27 (4), 29–35. (in Chinese with English Abstract). doi:10.3321/j.issn:0253-2697.2006.04.006

Liang, Z., Zhou, Y. Q., Wang, R., Liu, C. G., Zhu, Z. J., and Zhang, D. B. (2016). Hydrocarbon accumulation characteristics of well Gaogu 4 coal-derived gas reservoir in eastern Linqing Depression. *Coal Geol. Explor.* 44 (04), 46–53. (in Chinese with English Abstract).

Liu, D. M., Liu, Z. S., and Cai, Y. D. (2020). Research progress on accumulation mechanism and formation geological conditions of coalbed methane. *Coal Sci. Technol.* 48 (10), 1–16. (in Chinese with English Abstract). doi:10.13199/j.cnki.cst.2020.10.001

Liu, H. J., Jia, Y. R., Long, Y. Z., and Wang, H. W. (1987). The features of the barrier island systems of the epeiric sea and their event deposits of coal bearing formations in Carboniferous of North China. *Acta Geol. Sin.* 5 (3), 73–80. (in Chinese with English Abstract).

Liu, S. L., and Guo, J. P. (2003). Igneous rock features and its influence on coal seam and coal quality of Huanghebei coalfield,Shandong Province. *Coal Geol. China* 15 (6), 14–15. (in Chinese with English Abstract). doi:10.3969/j.issn.1674-1803.2003.06.005

Ma, Y. S., and Tian, H. Q. (2006). *A comprehensive study of deep sequence paleogeography and petroleum geology in the northern part of North China basin*. Beijing: Geological publishing house. (in Chinese with English Abstract).

Meng, Y. R. (2011). *Existent features and resource assessment of coalbed methane in Shandong Province – take Huanghebei and adjacent region for example*. Qingdao, China: Shandong University of Science and Technology, 42. (in Chinese with English Abstract).

Miao, F. B., Peng, Z. Q., Wang, Z. X., Zhang, B. M., Wang, C. S., and Gong, L. (2021). Brittleness characteristics and influencing factors of marine shale of niutitang Formation in xuefeng region: A case study of well XZD-1. *Geol. China* 2021, 1–18. (in Chinese with English Abstract). Available at: http://kns.cnki.net/kcms/detail/11.1167.P.20210913.1540.010.html.

Miu, J. J. (2008). *Analysis of the secondary hydrocarbon-generation mechanism and potential of the Carboniferous-Permian coal-measure source rocks in Jiyang-Linqing Depression*. Chengdu: Chengdu University of Technology. (in Chinese with English Abstract).

Ni, P. S., Long, Q., Cheng, T., Hu, Z. P., and Chen, F. K. (2013). Geochemistry and Sr-Nd-Pb isotopic composition of late mesozoic intermediate-basic rock in western Shandong block. *J. Earth Sci. Environ.* 35 (4), 62–76. (in Chinese with English Abstract).

Qin, J. Z., Li, Z. M., and Zhang, Z. R. (2005). Contribution of various coal measures source rocks to oil and gas reservoir formation. *Petroleum Explor. Dev.* 32 (04), 131–141. (in Chinese with English Abstract).

Qin, Y. (2021). Research progress and strategic thinking of coal-measure gas accumulation system and development geology. *J. China Coal Soc.* 46 (08), 2387–2399. (in Chinese with English Abstract). doi:10.13225/j.cnki.jccs.CB21.0719

Qin, Y. (2018). Research progress of symbiotic accumulation of coal-measure gas in China. *Nat. Gas. Ind.* 38 (4), 26–36. (in Chinese with English Abstract). doi:10.3787/j.issn.1000-0976.2018.04.003

Qin, Y., Shen, J., and Shen, Y. L. (2016). Joint mining compatibility of superposed gas-bearing systems: A general geological problem for extraction of three natural gases and deep CBM in coal series. *J. China Coal Soc.* 41 (1), 14–23. (in Chinese with English Abstract). doi:10.13225/j.cnki.jccs.2015.9032

Qin, Y., Xiong, M. H., Yi, T. S., Yang, Z. B., and Wu, C. F. (2008). On unattached multiple superposed coalbed-methane system: In a case of the shuigonghe syncline, zhijin-nayong coalfield, Guizhou. *Geol. Rev.* 54 (1), 65–70. (in Chinese with English Abstract). doi:10.16509/j.georeview.2008.01.015

Shao, L. Y., Dong, D. X., Li, M. P., Wang, H. S., Wang, D. D., Lu, J., et al. (2014). Sequence-paleogeography and coal accumulation of the Carboniferous-Permian in the North China basin. *J. China Coal Soc.* 39 (8), 1725–1734. (in Chinese with English Abstract). doi:10.13225/j.cnki.jccs.2013.9033

Shao, L. Y., He, Z. P., and Lu, J. (2008). *Study on sequence stratigraphy and coal accumulation of Carboniferous - Permian in the west of circum bohai bay*. Beijing: Geological publishing house. (in Chinese with English Abstract).

Shen, J., Li, K. X., Zhang, H. W., Shabbiri, K., Hu, Q. J., and Zhang, C. (2021). The geochemical characteristics, origin, migration and accumulation modes of deep coal-measure gas in the west of Linxing block at the eastern margin of Ordos Basin. *J. Nat. Gas Sci. Eng.* 91, 103965. doi:10.1016/j.jngse.2021.103965

Shen, L. J., Zhu, Y. Z., and Gao, Z. J. (2020). Paimary study on geological characteristics of Litun rock mass in Qihe-Yucheng rich iron ore area in Shandong Province. *Shandong Land Resour.* 36 (2), 23–29. (in Chinese with English Abstract). doi:10.12128/j.issn.1672-6979.2020.02.004

Shen, L. J., Zhu, Y. Z., Wang, H. H., Li, S., Gao, Z. J., Zhang, X. B., et al. (2021). Geochemical characteristics and geological significance of Litun iron ore deposit in Qihe - Yucheng area, Shandong Province. *Geol. Rev.* 67 (1), 84–98. doi:10.16509/j/georeview.2021.01.007

Shen, Y. L., Qin, Y., Guo, Y. H., Yi, T. S., Shao, Y. B., and Jin, H. B. (2012). Sedimentary controlling factor of unattached multiple superimposed coalbed-methane system formation. *Earth Sci. – J. China Univ. Geosciences* 37 (3), 573–579. (in Chinese with English Abstract). doi:10.3799/dqkx.2012.064

Shen, Y. L., Qin, Y., Shen, J., and Gu, J. Y. (2017). Sedimentary control mechanism of the superimposed gas bearing system development in the Upper Palaeozoic coal measures along the eastern margin of the Ordos Basin. *Nat. Gas. Ind.* 37 (11), 29–35. (in Chinese with English Abstract). doi:10.3787/j.issn.1000-0976.2017.11.004

Sheng, Q. H., and Li, W. C. (2016). Evaluation method of shale fracability and its application in Jiaoshiba area. *Prog. Geophys. (in Chinese)* 31 (4), 1473–1479. (in Chinese with English Abstract). doi:10.6038/pg20160409

Shi, L. Q., Liu, T. H., Zhang, X. Y., Huang, J. Y., Zhang, W., and Zhao, S. Q. (2020). Origin type and generating mechanism of coal measure limestone gas: A case study of L1 limestone gas in the Taiyuan Formation of the shenzhou coal mine, eastern edge of the Ordos Basin, China. *Enery & Fuels* 34, 10904–10914. doi:10.1021/acs.energyfuels.0c02127

Wang, H. H., Shen, L. J., Wang, D. D., Zhu, Y. Z., Li, Z. X., Wang, Y. J., et al. (2021a). Study on mesozoic magmatic intrusion and paleozoic multi-mineral Genesis mechanism in Huanghebei coalfield, Shandong Province. *Coal Geology & Exploration* 49 (2), 83–92. (in Chinese with English Abstract). doi:10.3969/j.issn.1001-1986.2021.02.011

Wang, H. H., Yin, L. S., Zhu, Y. Z., Wang, D. D., Zhou, M. L., Zhang, X. B., et al. (2021b). Paleozoic lithofacies, paleogeography and coal measures source rock development in Huanghebei region. *Coal Geology of China* 33 (1), 13–21. (in Chinese with English Abstract). doi:10.3969/j.issn.1674-1803.2021.01.03

Wang, Z. Z., Li, Z. X., and Yu, J. F. (2003). Stratigraphic sequence correlation of Permo-Carboniferous system in Luxi and Jiyang area. *Coal geology & exploration* 31 (5), 1–3. (in Chinese with English Abstract).

Xie, Q. H., Zhang, Z. C., Hou, T., Santosh, M., Jin, Z. L., Han, L., et al. (2015). Petrogenesis of the Zhangmatun gabbro in the Ji'nan complex, North China Craton: Implications for skarn-type iron mineralization. *Journal of Asian Earth Sciences* 113, 1197–1217. doi:10.1016/j.jseaes.2015.03.040

Xu, H. Z., Zhou, X. K., Gao, J. H., and Wang, X. W. (2005). Reconstruction of early-middle triassic basin in north China and hydrocarbon generation in palaeozoic. *Oil & Gas Geology* 26 (3), 329–336. (in Chinese with English Abstract). doi:10.3321/j.issn:0253-9985.2005.03.011

Yan, J. P., Yan, Y., Si, M. L. Q., Wen, D. N., Wen, X. F., and Geng, B. (2015). Relationship between fracture characteristics and "five-property" of shale reservoir. *Lithologic Reservoirs* 27 (03), 87–93+132. (in Chinese with English Abstract).

Yang, C. H., Xu, W. L., Yang, D. B., Liu, C. C., Liu, X. M., and Hu, Z. C. (2005). Chronology of the jinan gabbro in Western Shandong: Evidence from LA-ICP-MS zircon U-Pb dating. *Acta Geologica Sinica* 26 (4), 321–325. (in Chinese with English Abstract).

Yang, Q. L. (2012). *A geochemical study of Early Cretaceous mafic intrusions in the southeastern North China Block*. Hefei: University of Science and Technology of China. (in Chinese with English Abstract).

Yang, Y., Yang, C., Zhang, C. Z., Tang, W. Q., and Li, Y. (2018). Evaluation and potential analysis of coal measures source rocks in huimin sag. *Journal of Xi'an Shiyou University (Natural Science)* 33 (3), 2350. (in Chinese with English Abstract). doi:10.3969/j.issn.1673-064X.2018.03.004

Yang, Z. B., Qin, Y., Chen, S. Y., and Liu, C. J. (2013). Controlling mechanism and vertical distribution characteristics of reservoir energy of multi-coalbeds. *Acta Geologica Sinica* 87 (1), 139–144. (in Chinese with English Abstract). doi:10.3969/j.issn.0001-5717.2013.01.014

Yang, Z. B., Yi, T. S., Li, G., Yan, Z. H., Geng, D. Y., Gao, W., et al. (2021). Reservoir-forming characteristic of marine coal-measure gas and its favorable development segments: Taking the carboniferous xiangbai Formation in well longcan 1 in weining,

north Guizhou as an example. *Journal of China Coal Society* 46 (08), 2454–2465. (in Chinese with English Abstract). doi:10.13225/j.cnki.jccs.CB21.0797

Yao, Y. B., Liu, D. M., Tang, D. Z., Tang, S. H., and Huang, W. H. (2007). Preservation and deliverability characteristics of coalbed methane, North China. *Petroleum Exploration and Development* 34 (06), 664–668. (in Chinese with English Abstract).

Yu, L. P., Cao, Z. X., and Li, Z. X. (2003). Organic geochemical characteristics of carboniferous-permian hydrocarbon source rocks in jiyang depression. *Geology-Geochemistry* 31 (04), 68–73. (in Chinese with English Abstract).

Yuan, X. X. (2014). *Recognition of multi-coalbed methane bearing system: A case study of coal-bearing strata of upper permian in western Guizhou*. Xuzhou: University of Mining and Technology, 89–126. (in Chinese with English Abstract).

Zhang, C. C., Peng, W. Q., Hu, C. Q., Li, Z., Gao, B. Y., Li, Z. M., et al. (2020). Characteristics and resource potential of main shale gas reservoirs in Shandong Province. *Acta Geologica Sinica* 94 (11), 3421–3435. (in Chinese with English Abstract).

Zhang, D. W., Li, Y. X., and Zhang, J. C. (2012). *Investigation and evaluation of shale gas resource potential in China*. Beijing: Geological Publishing House, 10–138. (in Chinese with English Abstract).

Zhang, K. (2017). *Study on physical properties of differentrank coal reservoir in the eastern margin of Ordos basin (dissertation)*. Beijing: China University of Geosciences, 24–25. (in Chinese with English Abstract).

Zhang, W., Lu, J., Li, Y. J., Wang, J. Y., and Shao, L. Y. (2010). Sequence stratigraphy and coal accumulation of the Carboniferous and Permian coal measures in southwestern Shandong Province. *Journal of Palaeogeography* 12 (1), 90–96. (in Chinese with English Abstract).

Zhang, Z. N., Cao, Y., Zhu, Y. Z., Pang, Z. S., Shen, L. J., Guan, J. Y., et al. (2022). Enrichment mechanism of iron in Dazhang skarn iron deposit, Shandong Province: Evidence from fluid inclusions and hydrogen-oxygen isotopes. *Mineral Deposits* 41 (1), 91–105. (in Chinese with English Abstract). doi:10.16111/j.0258-7106.2022.01.006

Zhao, Q. F. (2005). *On the thermal evolution and kinetics of hydrocarbon generation of late Paleozoic coal measure source rocks in Huimin Depression*. Guangzhou: The Graduate School of the Chinese Academy of Sciences. (in Chinese with English Abstract).

Zhao, X. G. (2007). *Analysis on existent condition of coal-bed methane in Huanghebei coalfield and adjacent region*. Qingdao: Shandong University of Science and Technology. (in Chinese with English Abstract).

Zhao, Y., Ma, M. Y., and Qu, Z. L. (2016). Analysis of main control factors and estimation of resource of coal bed gas in the Huanghebei coalfield, Shandong Province. *Shandong Coal Science and Technology* 177 (8), 173–174. (in Chinese with English Abstract). doi:10.3969/j.issn.1005-2801.2016.08.074

Zheng, S. J. (2016). *Source-reservoir-cap rock assemblages and sequence sratigraphic framework control in coal measures of Linxing area*. Xuzhou: China University of Mining and Technology. (in Chinese with English Abstract).

Zhou, P. M. (2015). *Research on forming mechanism of the primary gas reserviors of the C-P coal-bearing sequence in Jiyang Depression*. Xuzhou: China University of Mining and Technology. (in Chinese with English Abstract).

Zhu, Y. M., Hou, X. W., Cui, Z. B., and Liu, G. (2016). Resources and reservoir formation of unconventional gas in coal measure, Hebei Province. *Journal of China Coal Society* 41 (01), 202–211. (in Chinese with English Abstract). doi:10.13225/j.cnki.jccs.2015.9013

Zhu, Y. Z., Zhang, Z. N., Shen, L. J., Wang, H. H., Zhou, M. L., Zhang, X. B., et al. (2021). Geochronology and geochemistry of late mesozoic diabase in the Litun ore district, north China Craton. *Geological Journal* 56 (9), 4735–4746. doi:10.1002/gj.4211

Zou, C. N., Tao, S. Z., and Hou, L. H. (2014). *Unconventional oil and gas geology*. Beijng: Geological Publishing House, 274–306. (in Chinese with English Abstract).

Zou, C. N., Yang, Z., Huang, S. P., Ma, F., Sun, Q. P., Li, F. H., et al. (2019). Resource types, formation, distribution and prospects of coal-measure gas. *Petrol. Explor. Develop.* 46 (3), 451–462. doi:10.1016/S1876-3804(19)60026-1